Review1

I would like to thank the authors for the extensive revision of their manuscript, which I find to be considerably improved compared to the previous version. This is a very nice and thorough work which covers the little-studied topic of energy-balance modeling of a Tibetan Plateau glacier.

While the manuscript makes an excellent contribution to the current literature, I still have some concerns on some of its aspects.

Response: We thank the reviewer for the encouraging words and for recognizing the improvements made in our revision. We have taken all of the remaining concerns very seriously and have addressed them point by point in the revised manuscript.

The reviewer raised a fundamental concern about the dual-threshold framework, questioning whether it can truly characterize an extreme year from a short time series. We fully understand this skepticism. We wish to emphasize that we did not apply the framework directly to Sangqu Glacier without validation. Instead, we first validated it on five long-term glaciers representing the major climatic regimes of the Tibetan Plateau, including Xiao Dongkemadi, Qiyi, Ningchan No.1, Guliya, and Xiao Anglong. For each glacier, we calibrated the multiplier k using a portion of its own record and tested the framework's performance on the remaining independent years. The results consistently identified all documented extreme mass loss years across these glaciers, confirming its robustness and transferability. Only after this validation did we transfer the k-values derived from the climatically similar Xiao Dongkemadi Glacier to Sangqu Glacier. We have made this validation process much more explicit in Section 5.2 and have added clear caveats in Sections 5.2 and 6.2 that the three-year Sangqu record is insufficient for independent threshold derivation, and that the framework serves as a diagnostic aid rather than the primary evidence of extremity, which rests on multiple independent lines of support, including the neighbouring Xiao Dongkemadi in-situ record and satellite products.

On the bias in modelled englacial temperatures, the reviewer correctly noted that while the correlation is high, there is a systematic cold bias of several degrees. We have investigated this issue in depth and now provide a fuller explanation in Section 4.2. The cold bias mainly arises from three factors: the model does not account for penetrating shortwave radiation within the ice, the density-based thermal conductivity parameterization may not fully capture the thermal properties of snow/firn under the intense radiation environment of the central Tibetan Plateau, and the simplified initial conditions may not have reached full equilibrium. We cite studies by Mölg et al. (2008), Wheler and Flowers (2011), and Yang et al. (2021) to support this interpretation. More importantly, we quantified the impact of this bias on our mass balance results. The sensitivity of glacier-wide annual mass balance to effective thermal conductivity and heat capacity is only −9.9 and +10.5 mm w.e. a^{-1}, respectively, far smaller than the extreme mass loss observed in 2021/22 and its anomaly relative to the previous two years. Because the bias is systematic, its effect on interannual anomalies is even smaller. We have therefore concluded that this bias does not affect our identification or quantification of the extreme melt event.

Regarding the Dussaillant et al. (2025) dataset, we thank the reviewer for the correction. We now describe it accurately as a fusion product combining glaciological in-situ measurements with geodetic mass balance observations, rather than a purely geodetic estimate. We have reduced the emphasis placed on this product, treating it only as a coarse independent reference for the anomaly direction, and have explicitly noted its limitations in Sections 2 and 4.2. We have also revised Figure 2h to compare relative anomalies across datasets rather than absolute values, which is more meaningful for our argument.

We have also made a number of smaller improvements throughout the manuscript. We have rounded numbers to avoid spurious precision. We streamlined Section 6.1, removed the temporal qualifier "during 2021-2022" from its title, and shortened the section by focusing on the most relevant comparisons while eliminating repetitive case descriptions. We removed Section 6.3 entirely, as we agreed with the reviewer that it

had limited relevance to the core focus of this study. On the fixed glacier geometry assumption, we shortened the discussion considerably and now simply state in Section 6.2 that for a short-term three-year study this simplification has negligible impact, consistent with the findings of Leclercq et al. (2010) and Huss et al. (2010). We also added quantitative area change data for Sangqu Glacier from 2007 to 2022 in Section 2, as requested. Finally, we added relevant references to support the limitations discussed in Section 6.2, strengthening the academic grounding of our uncertainty discussion.

We believe these revisions, which range from methodological clarifications to quantitative sensitivity analyses and structural streamlining, have substantially addressed the reviewer's concerns. We are grateful for the detailed and constructive feedback, which has helped us produce a much stronger manuscript.

General Comments

Comment1: Statistical approach to characterize ‘extreme’ years from short-term time series: I am still not convinced that the statistical approach introduced here is able to characterize a year as being ‘extreme’ or not. This approach seems to be novel (no other studies using such approach are referenced) but is not validated on longer time series and is simply applied to the short time series. There is therefore no valid demonstration on the applicability of this approach. The manuscript remains very relevant in many aspects, but I believe that this approach and the characterization of the 2022 year as ‘extreme’ need to be either re-worked or removed.

Response: We thank the reviewer for raising this methodological concern. We fully agree that a novel framework requires rigorous validation. It should be noted that prior to applying the framework to the short-term record of Sangqu Glacier, we validated it on multiple long-term observational series, as presented in Sect. 5.2 (Figs. 5 and S4).

First, we do not directly apply the mean-standard deviation criterion. Instead, we use the longest mass balance record on the central TP—Xiao Dongkemadi Glacier (1989–present)—as a training set to establish a mathematical relationship between the

percentile-based threshold (10th percentile) and the mean-standard deviation criterion, thereby determining the plausible range of the multiplier *k* with observational constraints. Given that Sangqu Glacier is located in the same climatically similar region of the central TP, transferring the *k* values calibrated from Xiao Dongkemadi to Sangqu is reasonable.

Second, we independently applied the same validation procedure to four other glaciers with long-term records: Qiyi Glacier and Ningchan No. 1 Glacier in the Qilian Mountains (arid continental type), and Guliya Glacier and Xiao Anglong Glacier in the western Kunlun Mountains (hyper-arid cold type). For each glacier, we calibrated *k* using a portion of its own record and tested the framework's performance on the remainder, ensuring an independent assessment. These four glaciers cover the major climatic regimes of the TP. As shown in Figs. 5 and S4, the framework successfully identifies all documented extreme mass loss years for each glacier, demonstrating its robustness across different climatic settings.

Third, even without this statistical framework, independent satellite data also point to the exceptionality of 2021/22. As shown in Figs. S5 (Hugonnet et al., 2021) and S6 (Dussaillant et al., 2025), the 2021/22 mass loss was approximately twice the 2000–2019 annual average and 600–700 mm w.e. more negative than the 1976–2021 mean at the same grid cell. These independent lines of evidence, together with our model simulation (−919 mm w.e.) and statistical identification, consistently indicate that 2022 was an exceptionally extreme year in recent decades.

We have revised the first paragraph of Section 5.2 as follows:

To evaluate the robustness of our proposed dual-threshold framework across different climatic regimes and record lengths, we applied it to five glaciers with long-term mass balance observations on the TP (Fig 1a, Fig. 5, and Fig. S4). These five glaciers were selected to represent the major climatic regimes of the Tibetan Plateau: Xiao Dongkemadi Glacier in the central plateau (relatively humid, summer-accumulation type), Qiyi Glacier and Ningchan No. 1 Glacier in the northern Qilian Mountains (arid continental), and Guliya Glacier and Xiao Anglong Glacier in the western Kunlun Mountains (hyper-arid, cold). For each glacier, we calibrated the

multiplier k based on a portion of its own record and tested the framework's performance on the remainder, ensuring an independent assessment of its detection capability. The results demonstrate that the framework consistently identifies documented extreme mass loss years across all five glaciers (Fig. 5 and Fig. S4), confirming its robustness and transferability across diverse climatic settings. Given the climatic similarity between Xiao Dongkemadi and Sangqu glaciers, we then applied the k values derived from the former to the short-term record of Sangqu Glacier. This stepwise approach, first validating the framework on multiple long-term records and then transferring it to a data-scarce glacier, strengthens the credibility of our extreme event identification for Sangqu Glacier.

We have added a paragraph at the end of Section 5.2, as follows:

In addition, we have now added a clear and explicit disclaimer in the main text (Section 5.2) to address the reviewer's concern about methodological independence. We state that: 'We acknowledge that the three-year Sangqu record is insufficient to define independent extreme thresholds. The k-values transferred from Xiao Dongkemadi are therefore used not to claim statistical independence, but to provide a consistent reference that places the 2021/22 anomaly, already supported by independent evidence (Section 4.2), on a comparable scale with other datasets. This framework serves as a diagnostic aid, not as the primary evidence of extremity.' This revision makes it unequivocal that the dual-threshold framework plays a supporting role, while the core conclusion rests on the convergence of multiple independent lines of evidence.

We have also added a statement of limitations in Section 6.2, as follows:

Another limitation concerns the short length of the Sangqu mass balance record (only three years), which precludes the independent derivation of extreme thresholds from the glacier's own data. Our approach of transferring k-values from Xiao Dongkemadi (Section 4.4) mitigates this issue to some extent, yet the associated uncertainty should be borne in mind when interpreting the absolute classification.

Comment2: Bias in modeled englacial temperatures: the figure S3 used for validation shows a good relative agreement between measured and modeled englacial

temperatures (leading to a high R2). However, there is a bias of several °C between the two. The origin and more importantly the effect of this bias on the modelling results should be investigated further.

Response: We thank the reviewer for this keen observation. We agree that the bias in englacial temperatures requires further scrutiny, and we have analyzed it from two aspects: the origin of the bias and its impact on the modelling results.

1. Origin of the bias

The cold bias in simulated ice temperatures (i.e., simulated temperatures systematically lower than observed) is mainly attributable to the following factors:

(1) The model does not account for penetrating shortwave radiation (QPS) within the snow/ice. In the EBFM, net shortwave radiation is treated entirely as surface-absorbed heat, neglecting its volumetric heating effect within the snow/ice. In reality, part of the solar radiation, particularly in the visible band, can penetrate the glacier surface and be absorbed layer by layer at depths of centimeters to decimeters (Brandt & Warren, 1993; Bintanja & Van den Broeke, 1995), directly warming the subsurface. Mölg et al. (2008) demonstrated on Kersten Glacier, Kilimanjaro, that neglecting QPS under bare-ice conditions leads to significant cold biases in simulated ice temperatures at 0.5 m and 2 m depth (their Figure 4), which were eliminated upon introducing a penetrating radiation parameterization. They further noted that QPS can be neglected when the glacier surface is snow-covered (Brandt & Warren, 1993), but during the ablation season when bare ice dominates, neglecting QPS significantly affects the accuracy of englacial temperature profiles, resulting in systematic underestimation of subsurface temperatures. This is entirely consistent with the direction of the cold bias we observed.

(2) Simplified thermodynamic parameterization. The model uses density-based parameterizations of effective thermal conductivity (Östin & Andersson, 1991; Sturm et al., 1997), which are based on observations from specific regions. Under the strong solar radiation conditions of the central TP, the structure and thermal properties of snow/firn layers may be unique, such that observed ice temperatures may be higher

than model results based on standard conductivity parameterizations.

(3) Simplified initial conditions. In reality, ice/snow temperature distributions are influenced by long-term climatic conditions and may have memory effects. Our model was initialized with a simplified temperature profile and may not have reached full equilibrium within the limited simulation window, potentially contributing to the systematic cold bias.

2. Impact of the cold bias on mass balance results

Despite these biases, the key question is whether they affect our main conclusions.

First, Mölg et al. (2008) successfully eliminated the cold bias in ice temperatures by incorporating QPS (their Section 3.2.4 and Figure 4), confirming that radiative penetration is indeed an important factor in englacial temperature simulation. Through sensitivity analyses of instrument errors (eight sensitivity tests applying typical instrument errors to global radiation, relative humidity, air temperature, and wind speed), they estimated the uncertainty in modeled net mass balance at approximately ±95 mm w.e. (their Section 4.1). This uncertainty (~95 mm w.e.) accounts for only about 30% of the anomalous melt increase (317.8 mm w.e.) during the 2022 heatwave in our study.

Wheler and Flowers (2011) compared subsurface treatment methods of varying complexity and found that the most complex multi-layer model (including radiative penetration and meltwater refreezing) underestimated ablation by only 6%, whereas simply assuming a surface temperature of 0°C overestimated ablation by 29%, and an iterative scheme solving subsurface heat flux as a residual of the energy balance equation overestimated total ablation by 18%. Yang et al. (2021) similarly found for Urumqi Glacier No. 1 that coupling a surface energy-mass balance model with a multi-layer subsurface heat conduction model yielded englacial temperatures in good agreement with observations. They further quantified the effect of neglecting subsurface heat flux: assuming a surface temperature of 0°C would overestimate summer ablation by about 6%. This is highly consistent with Wheler and Flowers (2011), suggesting that even with uncertainties in ice temperature simulation, the

impact on total ablation is within 10%. Thus, even if our model has uncertainties of a similar magnitude, they would not affect the magnitude or nature of the extreme melt event.

Although the cold bias is systematic under mean climatic conditions, the possibility of its amplification under extreme heat cannot be entirely ruled out. However, given that the surface energy balance during heatwaves is dominated by radiation and turbulent fluxes—while the subsurface heat flux remains a minor component—the relative contribution of this bias to the total melt anomaly is expected to remain small. This is consistent with the findings of Wheler and Flowers (2011) and Yang et al. (2021), who reported that even with simplified subsurface treatments, total ablation uncertainty stays within ~10%.

More importantly, our own sensitivity analysis directly quantified the impact of ice temperature bias on mass balance estimates. According to our sensitivity results (Tables S2–S4), the glacier-wide annual mass balance has a sensitivity of −9.9 mm w.e. a^{-1} to effective thermal conductivity and +10.5 mm w.e. a^{-1} to heat capacity. This means that even large relative deviations in these parameters affect annual mass balance by only 10–20 mm w.e. In comparison, the extreme mass loss observed in 2021/22 (~920 mm w.e.) and its anomaly relative to the previous two years (~440–500 mm w.e.) are one to two orders of magnitude larger. The mass balance uncertainty introduced by ice temperature bias is therefore far smaller than the signal of the extreme melt event itself.

Even when incorporating the uncertainty of the most sensitive parameters (ice/snow albedo, ±0.03, corresponding to ~120–130 mm w.e. sensitivity), the estimated uncertainty in melt energy during the 2022 heatwave is 99.3 mm w.e. (Table S1), still far smaller than the anomalous melt increase of 317.8 mm w.e.

Notably, the ice temperature bias may partially cancel out in interannual comparisons. Because the bias is systematic and originates from parameterization schemes, its behavior during the 2022 heatwave and the reference period is consistent, so its impact on anomalies (departures) is much smaller than on absolute values.

In summary, we confirm that the bias in simulated englacial temperatures mainly arises from the neglect of radiative penetration, simplified thermodynamic

parameterization, and the absence of latent heat effects. Mölg et al. (2008) successfully eliminated the cold bias in their model by incorporating QPS, and the studies of Wheler and Flowers (2011) and Yang et al. (2021) demonstrate that including subsurface processes such as radiative penetration can achieve model accuracy within 10%, providing a clear direction for future model improvements. Meanwhile, through sensitivity analysis, we have demonstrated that the current ice temperature bias does not affect the core conclusion that 2021/22 was an extreme mass loss year, nor does it affect the reliable estimate of the anomalous melt amount (317.8 mm w.e.) during the 2022 summer heatwave.

Section 4.2 (added, revised):

The simulated englacial temperatures show a systematic cold bias compared to observations (Fig. S3). This cold bias may arise from the following factors: (i) the model does not account for penetrating shortwave radiation at the bare-ice surface (Bintanja & Van den Broeke, 1995; Mölg et al., 2008); (ii) the density-based thermal conductivity parameterization (Östin & Andersson, 1991; Sturm et al., 1997) may not fully capture the thermal properties of snow/firn layers under the high-radiation environment of the central TP; and (iii) the simplified initial conditions may not have reached full equilibrium. Mölg et al. (2008) found on Kilimanjaro that neglecting penetrating shortwave radiation leads to a significant cold bias in ice temperatures, which was eliminated after incorporating the process. Wheler and Flowers (2011) and Yang et al. (2021) also emphasized the importance of including subsurface processes such as radiative penetration. Nevertheless, our sensitivity analysis shows that this bias has limited impact on mass balance: the glacier-wide annual mass balance has sensitivities of −9.9 mm w.e. a^{-1} to effective thermal conductivity and +10.5 mm w.e. a^{-1} to heat capacity, far smaller than the extreme mass loss observed in 2021/22 and its anomaly relative to the previous two years. Moreover, because this bias is systematic, its effect on interannual anomalies is smaller than on absolute values, and thus it does not affect our identification or quantification of the extreme melt event.

Section 6.2 (added, revised):

Furthermore, the model does not account for penetrating shortwave radiation within the glacier, which may introduce uncertainty in simulating englacial temperatures (Mölg et al., 2008; Wheler and Flowers, 2011). However, because this study focuses on surface energy balance and total melt, and because bare-ice surface temperatures remain near the melting point during the ablation season, this simplification has limited impact on our total melt estimates. It should, however, be considered when analyzing englacial thermal conditions and processes such as meltwater refreezing in future work.

Line-by-line comments

Comment3: L209-210: Based on the high uncertainties on these variables, the decimals are likely not significant and these numbers should be rounded.

Response: We thank the reviewer for this careful observation. We fully agree and have rounded all such values throughout the manuscript.

Comment4: L209-210 & L541-542: It's wrong to say that Dussaillant et al. (2025) provide geodetic estimates – it's more a fusion between WGMS glaciological measurements and geodetic mass balance measurements. In this regard I would recommend not putting too much emphasis on the Dussaillant et al. (2025) data, which gives a rough estimate but also comes with strong limitations.

Response: We thank the reviewer for this important correction. We have revised the description of the Dussaillant et al. (2025) dataset to accurately reflect its nature as a fusion product combining WGMS glaciological measurements with geodetic mass balance observations, rather than a purely geodetic estimate. We fully agree that this dataset has inherent limitations and should not be overemphasized. In the revised manuscript, we have reduced the emphasis placed on this dataset, treating it only as a

coarse independent reference rather than a primary validation tool, and have explicitly noted its limitations in the main text (Sections 2 and 4.2).

Section 2 has been revised as follows:

A fused product combining glaciological in-situ measurements with geodetic mass balance observations (Dussaillant et al., 2025) suggests a long-term mass loss rate of approximately 515 mm w.e. yr^{-1} for Sangqu Glacier over the period 1957–2024, though such large-scale fusion products come with considerable uncertainties at the individual glacier scale.

Section 4.2 has been revised as follows:

The extreme mass loss in 2021/22 is supported by two independent lines of evidence. First, the in-situ mass balance at the neighbouring Xiao Dongkemadi Glacier ranks as the third most negative in its nearly 30-year record, falling 619.5 mm w.e. below the 1989–2021 mean (Zhu et al., 2026a). Second, the coarse satellite-informed product of Dussaillant et al. (2025) shows a negative anomaly of 755.2 mm w.e. relative to the same reference period.

Comment5: L538-540: It doesn't really matter whether the glacier-wide mass balance of two glacier agrees as the mass turnover could still be very different. In your particular case what's important is to see if the mass losses relative to other years align for the 2 glaciers (i.e. both have unusually high mass loss). The same goes for the comparison with Dussaillant et al. (2025). Similarly, current Fig. 2h doesn't bring much and it would be more interesting to look at the relative temporal changes.

Response: We fully agree that comparing absolute mass balance values between different glaciers is of limited meaning, because their area, aspect, and mass turnover rates differ. What matters for our argument is the relative anomaly—that is, whether 2021/22 is anomalously negative relative to each glacier's own recent mean. We have

updated Fig. 2h accordingly, to show a comparison of relative anomalies across the different datasets.

Section 2 has been revised as follows:

A fused product combining glaciological in-situ measurements with geodetic mass balance observations (Dussaillant et al., 2025) suggests a long-term mass loss rate of approximately 515 mm w.e. yr^{-1} for Sangqu Glacier over the period 1957–2024, though such large-scale fusion products come with considerable uncertainties at the individual glacier scale.

Section 4.2 has been revised as follows:

The extreme mass loss in 2021/22 is supported by two independent lines of evidence. First, the in-situ mass balance at the neighbouring Xiao Dongkemadi Glacier ranks as the third most negative in its nearly 30-year record, falling 619.5 mm w.e. below the 1989–2021 mean (Zhu et al., 2026a). Second, the coarse satellite-informed product of Dussaillant et al. (2025) shows a negative anomaly of 755.2 mm w.e. relative to the same reference period.

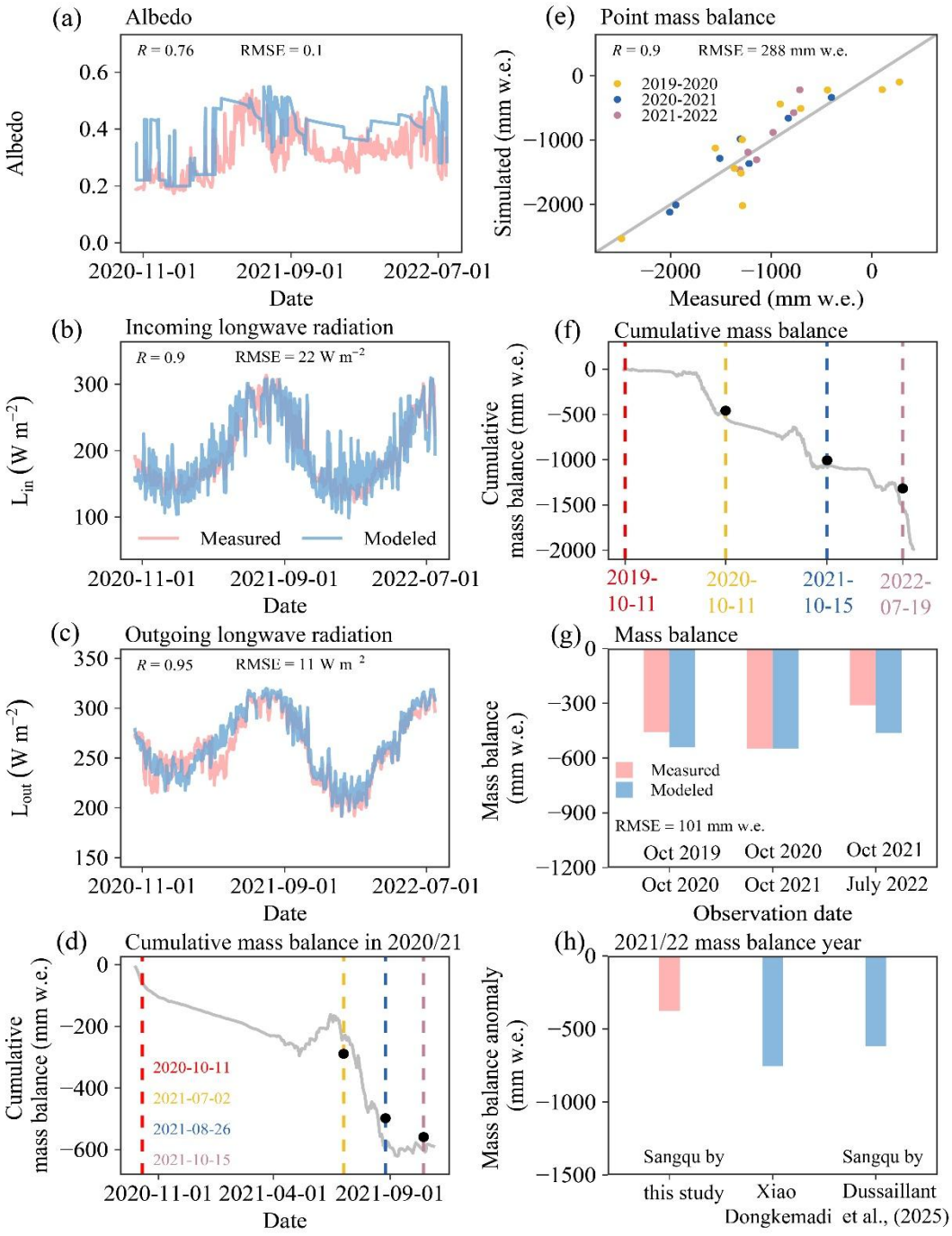


Figure 2. Comparison between observations and simulations of (a) albedo, (b) L_{in}, (c) L_{out}, (d) glacier mass balance from June to September 2021, (e) point mass balance at different elevations, (f) accumulation mass balance, and (g) glacier-wide mass balance for the periods 2019/20, 2020/21, and from October 2021 to July 2022. (h) Comparison of simulated 2021/22 mass balance anomaly for Sangqu Glacier (anomaly relative to 2019/20–2020/21 average) with observed anomaly for Xiao Dongkemadi Glacier and the anomaly for Sangqu Glacier from Dussaillant et al. (2025), with the latter two anomalies referenced to the 1989–2021 average.

Comment6: Section 6.2: no need to specify 'during 2021-2022' in the title since the extreme years in the other regions occur in different years. This new section is nice albeit a bit long, I would recommend some shortening.

Response: We thank the reviewer for the positive feedback on Section 6.2 and for the constructive suggestion to shorten it. We have removed the temporal qualifier "during 2021-2022" from the title and have substantially shortened the section by approximately 30%, focusing on the most relevant comparisons and eliminating repetitive descriptions of individual case studies. The core message—that extreme glacier melt events across global mountain regions share common driving mechanisms—has been retained and is now more prominent.

The revised Section 6.1 is shown below:

6.1 Comparison with extreme glacier mass loss events in other regions

Extreme mass loss events have been observed across diverse mountain glaciers, including the Swiss and Austrian Alps (Cremona et al., 2023; Voordendag et al., 2023; Van Tiel et al., 2026), Svalbard (Bernard and Friedt, 2025), the Pyrenees (Izagirre et al., 2024), the Tien Shan (Xu et al., 2024), western North America (Menounos et al., 2025), the central TP (Zhu et al., 2024a), and New Zealand (Vargo et al., 2020). In the Swiss Alps, 2022 mass loss exceeded the 1991–2020 average by more than threefold, with meltwater compensating for precipitation deficits in basins with ~15% glacier cover (Van Tiel et al., 2026). The Pyrenees lost nearly 40% of their glacier area between 2020 and 2023, with thinning rates triple those of the previous decade (Izagirre et al., 2024). Western North American glaciers lost 12% of their mass during 2021–2024, double the rate of 2010–2020 (Menounos et al., 2025). Central TP glaciers experienced anomalous early spring melting, typically part of the accumulation season (Zhu et al., 2024a).

These events share common drivers. Anomalous large-scale circulation, such as a weakened and northward-shifted westerly jet, creates conditions for persistent warmth (Zhu et al., 2024a). Record summer heatwaves, often combined with winter snow deficits, provide ample melt energy (Menounos et al., 2025; Xu et al., 2024). This is

reflected in increased incoming shortwave radiation and enhanced sensible heat flux (Thibert et al., 2018). The resulting earlier snowmelt exposes darker ice, reducing albedo and amplifying melt—a feedback loop further intensified by impurities like black carbon or dust (Menounos et al., 2025; Van Tiel et al., 2026). Liquid precipitation can destabilize snowpack, lengthening the melt season (Bernard and Friedt, 2025), while winter snow deficits advance ice exposure (Voordendag et al., 2023). Attribution studies confirm that anthropogenic warming has made such extreme years significantly more likely (Vargo et al., 2020).

These findings highlight the urgent need for systematic research into the increasing frequency of extreme glacier melt events and their downstream hydrological and hazard implications.

Comment7: L1354: Do you mean 'more than' 15%?

Response: We thank the reviewer for this careful check. We consulted the original text of Van Tiel et al. (2026) and confirmed that the authors used the phrasing "around 15% glacierization" (see their Abstract) and "15–20% glacier coverage" (see their Section 5.3), i.e. approximately 15% glacier cover. We have revised the wording in our manuscript to "~15% glacier cover" and added the temporal qualifier "during summer" to more accurately reflect the original meaning.

Section 6.1 has been revised as follows:

In the Swiss Alps, 2022 mass loss exceeded the 1991–2020 average by more than threefold, with meltwater compensating for precipitation deficits in basins with ~15% glacier cover (Van Tiel et al., 2026).

Comment8: L1397: No, the extreme years are not all happening in 2021-2022

Response: We thank the reviewer for this correction. We agree that the original wording

was ambiguous and could have led readers to assume that all extreme years occurred in 2021–2022. We have removed this phrasing from the main text and instead present the information as a regional listing, avoiding any misleading temporal constraint. Please see Section 6.2.

Comment9: Section 6.3: I find this section to have limited relevance here as it is not tied to the study itself. Consider removing it altogether (possibly keeping some of these elements for the introduction).

Response: We thank the reviewer for this suggestion. We agree that Section 6.3 had limited relevance to the core focus of our study and have removed it accordingly.

Comment10: L1493 & following paragraph: not accounting for glacier geometry changes is unlikely to be a strong limitation at such short temporal scales. This paragraph should be removed or considerably shortened.

Response: We thank the reviewer for this suggestion. We agree that glacier geometry changes are unlikely to be a strong limitation at the short temporal scale of this three-year study. Accordingly, we have removed the lengthy discussion and retained only a brief statement in Section 6.2, as follows:

"In addition, the model assumes fixed glacier geometry and does not account for the effects of area retreat or surface lowering on mass balance. However, for a short-term (three-year) study, this simplification has a negligible impact, as glacier area and surface elevation changes over such a brief period are minimal. This is also consistent with the findings of Leclercq et al. (2010) and Huss et al. (2010), who demonstrated that the opposing effects of retreat and surface lowering largely cancel each other out over longer timescales."

The quantitative area change data requested by Reviewer 2 (Comment 7) have been added to Section 2, where we now report the glacier area reduction from 18.04

km² (2007) to 16.34 km² (2022). We believe this revision appropriately addresses both reviewers' concerns.

Comment11: Section 6.4: this updated section on limitations is nice and reads well, however it lacks references to other studies that have investigated some of these aspects.

Response: We have added the relevant references in Section 6.2.

Review2

The paper uses in situ data (AWS since Oct 2020, mass balance stakes since Oct 2019) and an energy-mass balance model (EBFM) to study extreme melt on Sangqu Glacier during the 2022 heatwave. The authors also propose a "dual-threshold" method to find extreme mass loss years in short time series, tested it on other TP glaciers with longer records. The study concludes 2021/22 was an extreme mass loss year, driven by lower albedo, higher incoming longwave radiation, and higher sensible heat flux, linked to changes in the Western Pacific Subtropical High, South Asian High, and the westerly jet. While I think the study is a valuable contribution, I believe it can benefit a lot from more clarity. In its current form it is hard to reproduce. As a very general comment, I believe tables could guide the reader at many places(e.g. when the energy balance values are reported of the model, or when the climate and glacier variables are introduced in the beginning), as well as a flowchart that summarizes the methodology and especially what was available and used when.

Response: We thank the reviewer for the thoughtful and constructive assessment, and we have taken each major point seriously in preparing the revised manuscript.

To improve clarity and reproducibility, we substantially reorganized the methodology section (Sections 4.1–4.4) to present a clear stepwise workflow. This revision explicitly states what data were available, for which periods, and how they were used, from ERA5 downscaling and model calibration to heatwave definition and the dual-threshold framework. We believe this restructuring, together with the expanded supplementary tables (Tables S1–S4) that now summarize the sensitivity of all key parameters, provides readers with a transparent roadmap. We also added the anomaly values directly onto Figures 6 and S7, and clarified the heatwave periods in Figure 3g, which serves a similar guiding function as a table in a more concise visual form. We chose not to add a separate flowchart, as we felt the reorganized text and enhanced figures already convey the workflow clearly, but we remain open to adding one if the reviewer considers it necessary.

On the more critical technical issues, we fully acknowledge the data limitations raised by the reviewer. The AWS observations indeed cover only up to July 2022, meaning that the longest and most intense heatwave of the summer (4–29 August) falls within the period reconstructed from downscaled ERA5 data. We have added a dedicated paragraph in Section 6.2 to state this limitation transparently and to explain that we used all available observations, including four radiation components, stake measurements, and glacier-wide mass balances, to calibrate and validate the model through a multi-objective optimization algorithm (NSGA-II). We also point out that the conclusion of extreme mass loss is further supported by independent in-situ data from the neighbouring Xiao Dongkemadi Glacier and by satellite-informed products. Regarding the assumption of spatially uniform wind speed and relative humidity from a single AWS, we have clarified in Sections 4.1 and 6.2 that this follows common practice in data-scarce mountain environments. Sensitivity tests indicate that the resulting uncertainty in annual mass balance (about −55 to +8 mm w.e.) is minor compared to the observed extreme loss.

Concerning the dual-threshold method, we appreciate the reviewer's scrutiny. In Section 5.2 we now emphasize that this framework was first validated on five long-term glaciers across different climatic regimes of the Tibetan Plateau, demonstrating its ability to consistently identify documented extreme years. Only then was it transferred to Sangqu Glacier using k-values derived from the climatically similar Xiao Dongkemadi Glacier. We also added a clear caveat in Sections 5.2 and 6.2 that the three-year Sangqu record is insufficient for independent threshold derivation, and that the framework serves as a diagnostic aid rather than the primary evidence of extremity, which rests on multiple independent lines of support. We have also justified our use of daily mean temperature in the Standardized Heatwave Index by referencing the original method and explaining that daily mean better captures the cumulative effect of multi-day heatwave conditions relevant to glacier melt. In Section 4.3 we clarified that the three heatwaves are distinct events separated by intervening periods where the index dropped below the threshold.

On the energy balance calculations, we corrected a typo in the anomaly value of QG and now report consistent component anomalies that sum to the total melt energy increase of approximately 30 W m^{-2}. We also reordered the drivers in the abstract and conclusions to reflect the actual magnitudes, listing increased incoming longwave radiation and enhanced sensible heat flux before reduced albedo. We clarified that the 14 W m^{-2} increase refers to net longwave radiation, while the physically active driver we emphasize is the 20 W m^{-2} increase in incoming longwave radiation. For the circulation analysis, we added three new lines of evidence to move beyond a descriptive account. We analysed the Global Wave Train Index (GTI) and the South Asian High north-south displacement index (NSI), calculated their Pearson correlations with SHI over 1992–2022 ($r = -0.5$ for GTI and $r = 0.42$ for NSI, both $p < 0.05$), and explicitly compared the circulation configurations of 2022 with those of the non-extreme years 2020 and 2021. The results show that the exceptional 2022 signal arises from the synergistic combination of weakened westerlies and a strongly northward-shifted SAH, a pattern not present in the other two years. These analyses are now fully presented in Section 5.4 and Figures 7–8.

Finally, we have streamlined the discussion sections, removed the less relevant subsection on general circulation background, and added appropriate references to support the limitations discussed in Section 6.2. We believe these revisions have substantially strengthened the clarity, reproducibility, and scientific robustness of the manuscript. We are grateful to the reviewer for guiding us toward these improvements.

Main comments

Comment1: The biggest heatwave period is ERA5-based, not AWS-based. The AWS only has real measurements through July 2022, but the longest and most intense heatwave (4-29 August) falls entirely in the reconstructed Aug-Sep 2022 period. So the period driving their main "extreme melt" result has no real ground truth behind it, only RF-downscaled ERA5 data. This deserves to be stated directly in the discussion and generally could receive more attention.

Response: We fully agree with the reviewer. We have added a dedicated paragraph in Section 6.2 to directly and transparently address this data gap. In that paragraph, we clearly state that: (1) the AWS observations only cover the period up to July 2022, so the meteorological forcing for August–September is entirely based on downscaled ERA5 reanalysis data without concurrent in-situ validation; (2) despite this data gap, we have used all available observations to rigorously calibrate the model, including the four radiation components from the AWS, in-situ mass balance measurements at different elevations, and glacier-wide annual mass balances. Key parameters of the EBFM were calibrated using a multi-objective optimization algorithm (NSGA-II), and the model was validated at multiple scales against independent observations (Fig. 2), ensuring that it accurately simulates the energy and mass exchange processes over the glacier during the study period; (3) on this basis, we applied the rigorously validated model to the entire study period from October 2019 to September 2022, and the results represent the most reliable estimates under the current data constraints; (4) moreover, the conclusion of extreme mass loss in 2021/22 is further supported by two independent lines of evidence. The in-situ mass balance at the neighbouring Xiao Dongkemadi Glacier ranked as the third most negative in its nearly 30-year observational record, 619 mm w.e. below the 1989–2021 mean (Zhu et al., 2026a). In addition, multi-source satellite remote sensing products (Dussaillant et al., 2025) consistently show a strongly anomalous signal over the Sangqu Glacier region in 2021/22. We believe that this addition not only provides a candid assessment of the data limitation but also fully demonstrates the methodological efforts we have made to minimize its impact, thereby substantially enhancing the transparency and scientific rigor of the manuscript.

In Section 6.2, we add:

A further limitation concerns the meteorological forcing for August–September 2022. The AWS measurements cover only the period up to July 2022, meaning that the longest and most intense heatwave of the summer (4–29 August) falls entirely within the reconstructed period based on downscaled ERA5 data, without concurrent in-situ validation. To minimize this data gap, we used all available observations to calibrate

and validate the model, ensuring its reliability over the study period (Fig. 2). Importantly, the conclusion of extreme mass loss in 2021/22 is independently supported by in-situ observations from the neighbouring Xiao Dongkemadi Glacier (Zhu et al., 2026a) and by satellite remote sensing products (Dussaillant et al., 2025), which consistently show a strongly anomalous signal over the Sangqu Glacier region.

Comment2: Single AWS, uniform wind/RH assumption. Wind speed and relative humidity from one station are assumed the same across the whole glacier. The assumption is backed with other studies, however a quick check revealed that comparability might be limited, I think some clarification should be provided.

Response: We agree with the reviewer that this assumption requires clearer justification. Our treatment follows common practice in distributed energy-balance modelling for data-scarce mountain glaciers (e.g., Hock & Holmgren, 2005). Given the relatively small area and limited elevation range of Sangqu Glacier, the spatial variability of relative humidity is generally modest at this scale. Wind speed may vary with local topography, but applying the single-station record as a background field over the entire glacier remains the most feasible approach under the current observational constraints. More importantly, we performed a sensitivity analysis by perturbing the turbulent exchange coefficient by ±10%. The resulting annual mass balance change ranged from −55 to 8.3 mm w.e., which is substantially smaller than the annual mass loss rate of Sangqu Glacier, confirming that the uncertainty introduced by this assumption has a negligible impact on our core conclusions. We have added a detailed description of these sensitivity and uncertainty analyses for the key parameters in the turbulent flux parameterization to Section 4.2.

We have acknowledged this limitation in Section 4.2, as follows:

The results of the sensitivity tests are presented in the supplementary materials (Tables S1-S4). The glacier-wide mass balance of the Sangqu Glacier exhibits particularly high sensitivity to ice and snow albedo. Specifically, the sensitivities to

parameters related to snow, firn, and ice albedo are 123.2, 114.7, −0.3, and 126.3 mm w.e. a^{-1}, respectively. The temperature lapse rate shows a sensitivity of -141.4 mm w.e. a^{-1}. The background turbulent exchange coefficient and turbulent flux coefficient yield sensitivities of 8.3 and −55 mm w.e. a^{-1}, respectively. In comparison, the sensitivity of the glacier-wide mass balance to the rain-snow temperature threshold and precipitation gradient are relatively minor, at 0.5 and −2.2 mm w.e. a^{-1}, respectively. The sensitivity to the aerosol transmissivity coefficient is −20.2 mm w.e. a^{-1}. The glacier-wide annual mass balance has a sensitivity of −9.9 mm w.e. a^{-1} to effective thermal conductivity and +10.5 mm w.e. a^{-1} to heat capacity.

We have acknowledged this limitation in Section 6.2, as follows:

In addition, the use of a single AWS to drive the distributed model assumes spatially uniform wind speed and relative humidity across the glacier. While this simplification follows common practice in data-scarce mountain environments, it may not fully capture local topographic effects on wind fields. However, our sensitivity analysis indicates that the resulting uncertainty in annual mass balance is minor relative to the observed mass loss (Section 4.2).

Comment3: Not sure if I get it right with the definition of the dual-threshold method. I assumed it was explicitly designed to work for short-records. However, it turned out that the k value was borrowed from another glacier. Sangqu's own record is too short to calibrate the k multiplier, so k is taken from Xiao Dongkemadi instead. This means the "extreme year" classification for Sangqu is not really independently derived, it depends on transferring a parameter from elsewhere? Doesn't this significantly limit the claims?

Response: We thank the reviewer for raising this critical point, which was indeed a central challenge in our method design. With only three years of observations at Sangqu Glacier, we recognize that it is statistically impossible to define "extremes" independently. Our approach therefore proceeded differently: we first established the

identification rules on a glacier with a long-term record and then transferred them to a short-record glacier with a similar climatic background. We wish to clarify that we did not attempt to make the short record "self-demonstrating"; rather, we sought a defensible method given limited data.

We selected Xiao Dongkemadi Glacier as the reference for two reasons. First, the two glaciers are both located in the Central Tanggula Mountains, approximately 90 km apart, and share highly similar climatic conditions. Second, Xiao Dongkemadi has nearly 30 years of continuous observations, the longest mass balance record on the central TP. We validated the stability of the multiplier *k* on this glacier and then transferred it to Sangqu.

We fully understand the reviewer's concern that the classification for Sangqu is not entirely independent. Accordingly, we present the dual-threshold framework as a diagnostic tool that complements other lines of evidence, rather than as the sole basis for our conclusions. In fact, the identification of 2021/22 as an extreme mass loss year rests primarily on independent evidence: the in-situ mass balance at Xiao Dongkemadi ranked as the third most negative in its nearly 30-year record, and multiple satellite products show consistent signals. The value of the framework lies in providing a normalized reference that makes the classification of "extreme" methodologically traceable.

We have revised the first paragraph of Section 5.2 accordingly to reflect these points.

To evaluate the robustness of our proposed dual-threshold framework across different climatic regimes and record lengths, we applied it to five glaciers with long-term mass balance observations on the TP (Fig 1a, Fig. 5, and Fig. S4). These five glaciers were selected to represent the major climatic regimes of the Tibetan Plateau: Xiao Dongkemadi Glacier in the central plateau (relatively humid, summer-accumulation type), Qiyi Glacier and Ningchan No. 1 Glacier in the northern Qilian Mountains (arid continental), and Guliya Glacier and Xiao Anglong Glacier in

the western Kunlun Mountains (hyper-arid, cold). For each glacier, we calibrated the multiplier k based on a portion of its own record and tested the framework's performance on the remainder, ensuring an independent assessment of its detection capability. The results demonstrate that the framework consistently identifies documented extreme mass loss years across all five glaciers (Fig. 5 and Fig. S4), confirming its robustness and transferability across diverse climatic settings. Given the climatic similarity between Xiao Dongkemadi and Sangqu glaciers, we then applied the k values derived from the former to the short-term record of Sangqu Glacier. This stepwise approach, first validating the framework on multiple long-term records and then transferring it to a data-scarce glacier, strengthens the credibility of our extreme event identification for Sangqu Glacier.

We have added a paragraph at the end of Section 5.2, as follows:

We acknowledge that the three-year Sangqu record is insufficient to define independent extreme thresholds. The k-values transferred from Xiao Dongkemadi are therefore used not to claim statistical independence, but to provide a consistent reference that places the 2021/22 anomaly, already supported by independent evidence (Section 4.2), on a comparable scale with other datasets. This framework serves as a diagnostic aid, not as the primary evidence of extremity.

We have also added a statement of limitations in Section 6.2, as follows:

Another limitation concerns the short length of the Sangqu mass balance record (only three years), which precludes the independent derivation of extreme thresholds from the glacier's own data. Our approach of transferring k-values from Xiao Dongkemadi (Section 4.4) mitigates this issue to some extent, yet the associated uncertainty should be borne in mind when interpreting the absolute classification.

Comment4: The index uses daily mean temperature, while other cited studies (Hua et al. 2023) use daily maximum. This choice could change the results I assume, also given the fact that max temperature often is the better predictor for melt-events!?

Response: We thank the reviewer for raising this important question regarding the

choice of temperature metric. Our selection was based on the following considerations.

First, the original formulation of the Standardized Heatwave Index (SHI) explicitly uses daily mean temperature. Raei et al. (2018) clearly stated in their methodology that "SHI and EHF methods employ average daily temperature." We adopted the same setting to maintain methodological consistency with the original approach.

Second, daily mean temperature is widely used in glacier mass balance studies. Across the Tibetan Plateau and global mountain glaciers, it is the most commonly adopted thermal metric. The positive degree-day method, based on daily mean temperature, is a classical approach for estimating glacier melt (Hock, 1999) and has been applied to glaciers in various climatic regimes. In glacier mass balance studies on the Tibetan Plateau, daily mean temperature is also the most commonly used thermal indicator. As a comprehensive measure of the day's thermal condition, it correlates well with the cumulative effect of glacier melt.

Third, we agree with the reviewer that daily maximum temperature is more sensitive to individual extreme melt days. However, our study focuses not on the peak intensity of single-day extremes, but on the continuous identification of heatwave windows—specifically, which periods exhibit multi-day temperature anomalies and where their onset and end dates lie. Daily mean temperature better reflects the cumulative effect of sustained heatwave conditions and avoids the interference of isolated anomalous hot days in determining event persistence. Furthermore, Hua et al. (2023) examined extreme heat in the middle reaches of the Yangtze River, which falls within the climatological definition of heatwaves, whereas our study focuses on the thermal conditions at the glacier surface and their cumulative impact on melt—two distinct physical contexts that justify different metric choices.

We have added the above clarification to the Methods section (Section 4.3) of the revised manuscript to justify our choice of temperature metric.

“We follow Raei et al. (2018) in using daily mean air temperature for the SHI calculation, as the original method employs this metric. From a glaciological perspective, daily mean temperature is preferred over daily maximum for two reasons. First, glacier melt responds to the cumulative thermal forcing over the entire diurnal

cycle, and daily mean temperature better represents the total energy available for melt over multi-day heatwave events. Second, the widely used positive degree-day method for glacier mass balance modeling is traditionally based on daily mean temperatures (Hock, 2003), making this choice consistent with standard glaciological practice for capturing sustained melt anomalies rather than isolated peak temperature extremes."

Raei, E., Nikoo, M. R., AghaKouchak, A., Mazdiyasni, O., and Sadegh, M.: GHWR, a multi-method global heatwave and warm-spell record and toolbox, Sci. Data, 5, 180206, https://doi.org/10.1038/sdata.2018.206, 2018.

Hock, R.: Temperature index melt modelling in mountain areas, J. Hydrol., 282, 104–115, https://doi.org/10.1016/S0022-1694(03)00257-9, 2003.

Comment5: Are you confident that we can split the 2022 summer period into 3 distinct heatwaves (fig. 3) or whether we do not just have an extended/anomaly warm season?

Response: We thank the reviewer for raising this question, and we fully understand the concern.

Our study focuses on the event scale—specifically, the extreme melt pulses driven by individual heatwaves—rather than the seasonal mean state. Within the ablation season (June–September), we identified heatwave events objectively using the Standardized Heatwave Index (SHI), which defines a heatwave when daily mean temperature exceeds the climatological mean for the same calendar day over the past 30 years, with the SHI remaining above the threshold for at least three consecutive days (Raei et al., 2018). Under this objective criterion, the three identified heatwave windows are separated by clear intervening periods during which the SHI dropped below the threshold and no longer met the heatwave definition.

We acknowledge that the entire 2022 ablation season was anomalously warm, with temperatures during the intervening periods also above the climatological mean. A more accurate description, therefore, is that the summer of 2022 featured a persistently warm background state with three distinct extreme heatwaves superimposed upon it—each meeting the SHI criteria in terms of both intensity and duration. These two characterizations are not contradictory: one describes the background state, the other

the extreme events embedded within it. To avoid potential misunderstanding, we have added this clarification to the revised manuscript and updated Fig. 3g to clearly indicate the identified heatwave events.

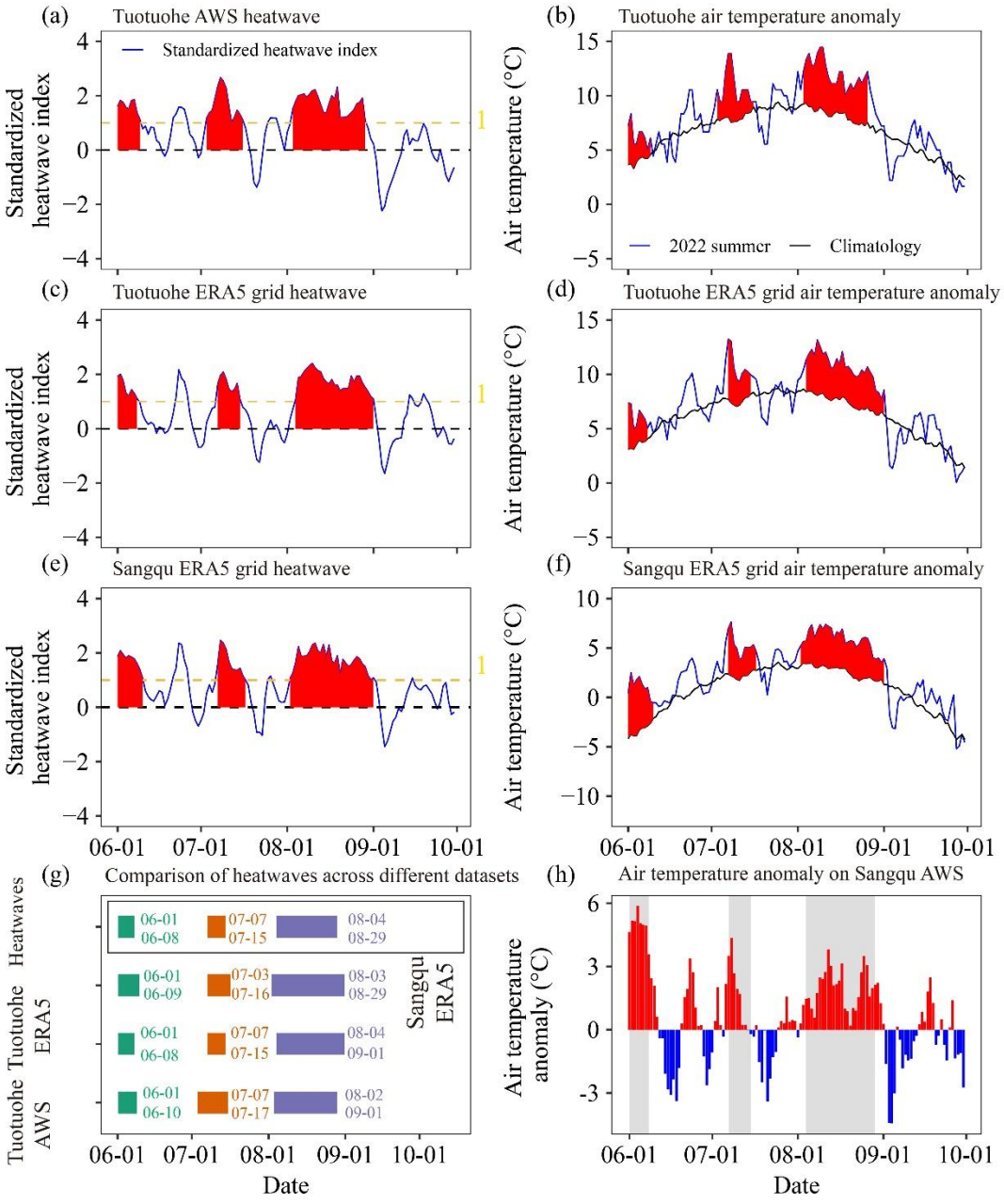


Figure 3. Identification of heatwave events from June to September 2022. Air temperature anomalies are calculated relative to the 1992–2021 climatology. (a, b) Heatwave events and corresponding temperature anomalies at the Tuotuohe meteorological station. (c, d) As in (a, b), but for the ERA5 grid cell containing the Tuotuohe meteorological station. (e, f) As in (a, b), but for the

ERA5 grid cell containing Sangqu Glacier. In panels (a), (c), and (e), the yellow line marks the standardized heatwave index threshold of 1; a heatwave is identified when the index exceeds this threshold for at least three consecutive days. (g) Comparison of heatwave events identified from the three datasets shown in (a), (c), and (e). (h) Summer (June–September) temperature anomalies at Sangqu Glacier in 2022 based on the identified heatwave events.

Comment6: Comparison with Dussaillant et al. (2025). Their model gives -919.8 mm w.e., in situ neighbor gives -881, but the satellite product gives -1278 mm w.e. That is a large gap (about 350+ mm w.e.) and I am wondering about the quality of the satellite product as the paper treats this as supporting evidence for an extreme year.

Response: We thank the reviewer for raising this important point. We agree that the large discrepancy between the satellite product and our model results (approximately 350 mm w.e.) warrants clarification.

We wish to clarify that we do not rely on the Dussaillant et al. (2025) product for its absolute mass balance value at the individual glacier scale. As we have stated in the manuscript, such large-scale fusion products come with considerable uncertainties at the individual glacier scale. We use this dataset not as a benchmark for the absolute mass balance of Sangqu Glacier, but only as an independent indicator of the regional anomaly pattern. Accordingly, in the revised manuscript we have removed the absolute value (−1278 mm w.e.) from the main text and refer only to the anomaly signal shown in the product.

What makes this product useful is that its anomaly field indicates a negative mass balance anomaly of −755.2 mm w.e. for the Sangqu region in 2021/22 (Fig. 2h). This independent, satellite-based signal points to a pronounced regional mass loss anomaly, rather than providing a precise absolute estimate for Sangqu Glacier. We cite it solely to corroborate the regional context of extreme anomaly.

A more direct and robust line of support for the extreme nature of 2021/22 comes from the in-situ mass balance at the neighbouring Xiao Dongkemadi Glacier, which ranks as the third most negative in its nearly 30-year record and is 619.5 mm w.e. below

the 1989–2021 mean (Zhu et al., 2026a). Given that the two glaciers are approximately 90 km apart, share the same climatic setting in the Central Tanggula Mountains, and have highly consistent climatic backgrounds, the anomaly recorded at Xiao Dongkemadi provides critical independent evidence for the extremity of Sangqu Glacier.

We have revised the relevant text accordingly in the manuscript, retaining the Dussaillant et al. (2025) product only as an indicator of the anomaly direction rather than as a source of absolute values.

Section 2 has been revised as follows:

A fused product combining glaciological in-situ measurements with geodetic mass balance observations (Dussaillant et al., 2025) suggests a long-term mass loss rate of approximately 515 mm w.e. yr^{-1} for Sangqu Glacier over the period 1957–2024, though such large-scale fusion products come with considerable uncertainties at the individual glacier scale.

Section 4.2 has been revised as follows:

The extreme mass loss in 2021/22 is supported by two independent lines of evidence. First, the in-situ mass balance at the neighbouring Xiao Dongkemadi Glacier ranks as the third most negative in its nearly 30-year record, falling 619.5 mm w.e. below the 1989–2021 mean (Zhu et al., 2026a). Second, the coarse satellite-informed product of Dussaillant et al. (2025) shows a negative anomaly of 755.2 mm w.e. relative to the same reference period.

Comment7: Fixed glacier geometry. Acknowledged as a limitation, but given the size of the reported mass loss, some comment on how much this could bias the melt estimate would help maybe (especially in the context of an extreme event)?

Response: The reviewer is correct. While we acknowledged this limitation, we did not provide a quantitative estimate of its potential bias, making it difficult for readers to

assess its actual impact on our conclusions. We have added the following analysis to the revised manuscript.

Regarding area change: the Second Chinese Glacier Inventory (based on 2006–2010 imagery) gives an area of 18.04 km² for Sangqu Glacier, while Sentinel-2 imagery yields 16.4 km² in 2020 and 16.34 km² in 2022. This reflects long-term retreat over approximately 14 years (2007–2022), rather than changes over the 2019–2022 study period. We do not have interannual area data, so the exact area change over these three years is unknown, but it is reasonable to assume that it is substantially smaller than the long-term change.

Regarding the temperature feedback from surface lowering: the 2021/22 mass loss of −919 mm w.e. corresponds to a mean surface lowering of approximately 1 m. Using a lapse rate of 0.6°C per 100 m, this elevation change would increase local air temperature by about 0.006°C, which would generate only negligible additional melt. We acknowledge that this estimate is approximate, as it depends on the assumed mean ice thickness.

More importantly, our core analysis focuses on the interannual anomalies—i.e., the differences between 2021/22 and the preceding two years. Because the bias introduced by the fixed-geometry assumption is systematic across all years, it largely cancels out in the differencing. Thus, even if the assumption introduces some bias in absolute mass balance estimates, its impact on the interannual anomaly—and therefore on our identification of 2021/22 as an extreme year—is substantially smaller.

The following description of Sangqu Glacier area changes has been added to Section 2:

The glacier area of Sangqu Glacier has undergone notable changes in recent decades. The Second Chinese Glacier Inventory (based on 2006–2010 imagery) recorded an area of 18.04 km² for Sangqu Glacier. By 2020, the glacier area had decreased to 16.4 km² (Xiao et al., 2025). Based on our own delineation from Sentinel-2 imagery acquired in 2022, the area further reduced to 16.34 km².

In Section 6.2, we discuss the limitations of assuming a fixed glacier geometry.

In addition, the model assumes fixed glacier geometry and does not account for the effects of area retreat or surface lowering on mass balance. However, for a short-term (3-year) study, this simplification has a negligible impact, as glacier area and surface elevation changes over such a brief period are minimal. This is also consistent with the findings of Leclercq et al. (2010) and Huss et al. (2010), who demonstrated that the opposing effects of retreat and surface lowering largely cancel each other out over longer timescales.

Comment8: Snow/ice density assumption (300/900 kg/m3): Mass balance is derived from stake height times a fixed density. 300 kg/m3 for snow is a simplification, real snow density on the TP varies a lot depending on on multiple aspects obviously. However, did the authors maybe do a simple sensitivity test with a plausible density range?

Response: We thank the reviewer for this suggestion. To address this concern, we conducted a sensitivity test using the 2019/20 mass balance year as an example. We recalculated the point mass balance at different elevations using alternative snow density values of 100, 200, and 400 kg/m³, compared to the baseline value of 300 kg/m³. The results show that the variations in point mass balance range from –35 to 70 mm w.e., depending on elevation and density assumption.

We have added the results of this sensitivity test in Section 3.2, and the results are as follows:

Taking the 2019/20 mass balance year as an example, sensitivity tests indicate that when snow density is changed from the baseline value of 300 kg/m³ to 100, 200, and 400 kg/m³ respectively, the point mass balance variations at different elevations range from –35 to 70 mm w.e.(Fig. S9).

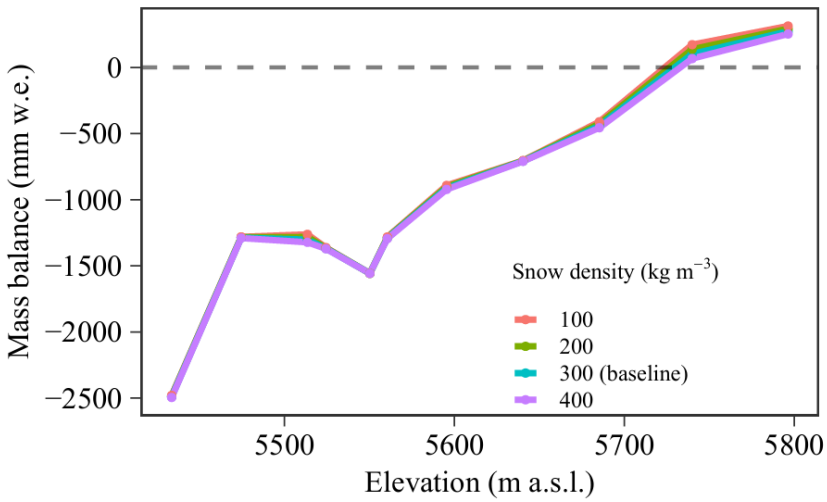


Figure S9. Sensitivity of point mass balance to snow density at different elevations for the 2019/20 mass balance year.

Comment9: Precipitation correction ratio: Am I right that only one single ratio (measured/ERA5) over the whole period was calculated and applied to reconstruct earlier years? The actual ratio value is never reported, and it is unclear if it varies by season. Since gauge undercatch usually differs between rain and snow, a single annual ratio is quite simplistic. I would assume this matters a lot and more sophisticated approaches would have been easy to implement?

Response: We thank the reviewer for this suggestion. We have recalculated the precipitation correction factors for each season, and the comparison between measured precipitation and ERA5 estimates for each season is shown in the figure below.

Based on the observed data at Sangqu Glacier from October 2020 to July 2022, winter (DJF) precipitation is extremely low, accounting for only 4.24% of the total precipitation during the overlap period. Even though the winter correction factor is high (5.34), its contribution to the annual total is very limited, with measured winter precipitation amounting to only approximately 35.5 mm out of the annual total of 837.1 mm (4.24%). The seasonal correction factors are 0.92 for spring, 0.96 for summer, 1.29 for autumn, and 5.34 for winter, yielding a precipitation-weighted annual average of 1.028, which is consistent with the single annual ratio.

We ultimately adopted the annual mean correction factor (1.028) for the following

reasons. First, Sangqu Glacier is a summer-accumulation type glacier, and winter precipitation accounts for only 4.24% of the annual total, making its contribution to the annual mass balance extremely limited. Second, during winter the glacier is in a quiescent state with negligible melt, so the accuracy of winter precipitation has a minimal impact on the simulation of the annual mass balance. Third, the unusually high winter correction factor (5.34) largely reflects the inherent difficulties of measuring solid precipitation in high-altitude cold regions, and applying such an extreme factor could introduce additional uncertainty.

We therefore consider the annual mean correction factor (1.028) to be more robust and reliable under the current data constraints.

Following the reviewer's suggestion, we have now explicitly included the seasonal correction factors (0.92, 0.96, 1.29, and 5.34) and the winter precipitation proportion (4.24%) in Section 4.1. This addition transparently justifies our use of the annual mean factor (1.028) and clarifies that the high winter ratio does not bias the annual reconstruction, as the glacier is largely inactive during that period.

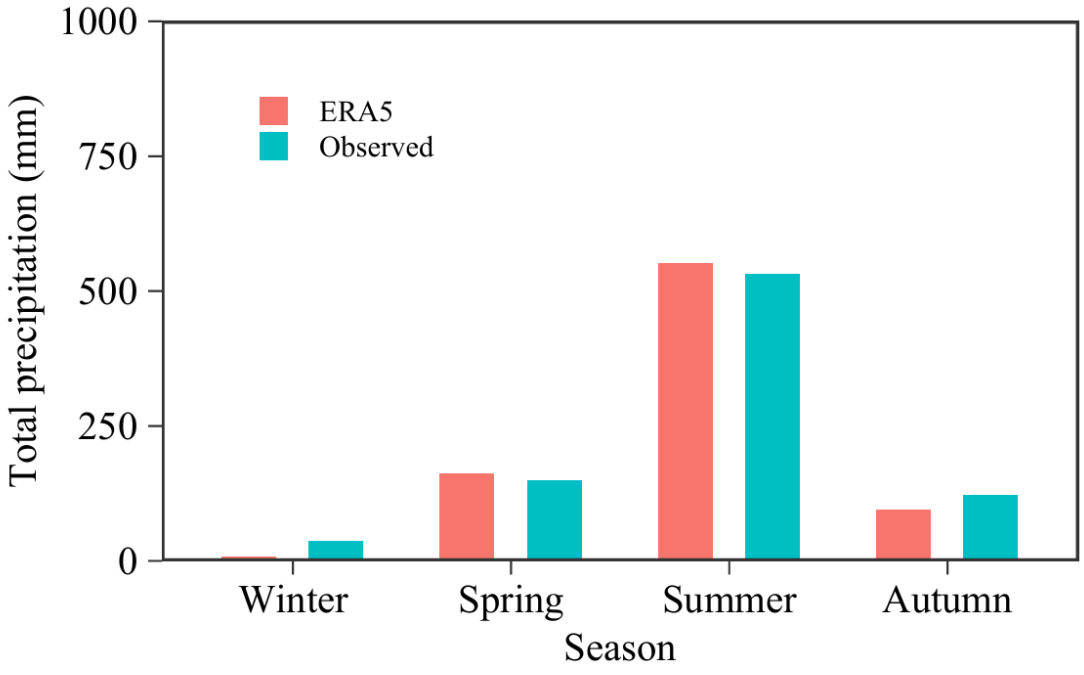


Figure 2. Seasonal comparison between ERA5 and in-situ precipitation measurements at Sangqu Glacier.

Comment10: Glacier outline year is not stated!? The authors cite the Second Chinese Glacier Inventory but never say which year the outline is from. This inventory is generally based on mid-to-late 2000s imagery, so there may be a real mismatch with the 2019-2022 study period, on top of the fixed-geometry issue already mentioned leading again, especially in an extreme year, to a significant bias?

Response: We thank the reviewer for pointing out this omission. We have now added the specific glacier outline years to the revised manuscript and have integrated this with our response to Comment 7 on the fixed-geometry assumption.

First, glacier inventory years and data sources.

The Second Chinese Glacier Inventory (Guo et al., 2015) is primarily based on Landsat imagery from 2006–2010, with the outline of Sangqu Glacier derived from an image acquired on 5 May 2007, recording an area of 18.04 km². The 2020 Tibetan Plateau Glacier Inventory (Xiao et al., 2025) gives an area of 16.4 km². In addition, we manually delineated the glacier boundary from Sentinel-2 imagery acquired on 3 June 2022, yielding an area of 16.34 km². Between 2007 and 2022, the glacier area decreased from 18.04 km² to 16.34 km², a retreat of approximately 1.70 km² (~9.4%), consistent with the ongoing glacier retreat trend in the Geladandong region. These details have been added to Section 3.3 of the revised manuscript.

Second, implications for mass balance estimates.

Regarding the direct effect of area change: the above data reflect long-term retreat over approximately 15 years (2007–2022), rather than interannual changes over the 2019–2022 study period. We lack interannual area data, but the change over the three-year study period is expected to be substantially smaller than the long-term trend.

Regarding the temperature feedback from surface lowering: the 2021/22 mass loss of −919 mm w.e. corresponds to a mean surface lowering of approximately 1 m. Using a lapse rate of 0.6°C per 100 m, this elevation change would increase local air temperature by only about 0.006°C, generating negligible additional melt.

More importantly, our analysis focuses on interannual anomalies among the three mass balance years (2019–2022), rather than on absolute mass balance values for any

single year. Systematic biases arising from the inventory year mismatch and the fixed-geometry assumption largely cancel out in the interannual differencing. Thus, the impact on our identification of 2021/22 as an extreme mass loss year is limited.

We have added the glacier outline sources and area data to Section 2, 3.3 and 6.2.

Comment11: Section 5.3 is hard to read. Every energy component's anomaly is reported as a separate sentence, pointing to different sub-panels across two figures (Fig 6 and Fig S7). A summary table with all component anomalies and their figure references would make this much easier to follow.

Response: We thank the reviewer for this excellent suggestion, which we fully accept. We agree that describing each energy component anomaly in separate sentences across two figures (Fig. 6 and Fig. S5) makes it difficult for readers to grasp the overall picture quickly. To address this, we have added the anomaly values directly in the figures for easier reading and interpretation.

Comment12: Which term is really the main driver is unclear from the text. Looking at the actual numbers: QH +17.0 W/m2, Lnet +14.0 W/m2, Snet +5.1 W/m2. So sensible heat flux is actually the largest term, not albedo/shortwave, even though the abstract lists "reduced albedo" first. The ranking in the text might be updated if considered valuable?

Response: We thank the reviewer for the careful reading. We would like to clarify a point that may have caused confusion. The 14.0 W m^{-2} mentioned by the reviewer is the anomaly in net longwave radiation, whereas the driver we list in the abstract is increased incoming longwave radiation — these two have distinct physical meanings.

Incoming longwave radiation is the longwave radiation emitted by the atmosphere toward the glacier surface; its enhancement directly reflects atmospheric warming and increased moisture content, representing an active energy input process. Net longwave radiation, by contrast, is the difference between downward and upward longwave radiation; an increase in net longwave radiation could result from an increase in

incoming longwave radiation or a decrease in outgoing longwave radiation. During the heatwave, incoming longwave radiation increased by 20 W m^{-2}, while outgoing longwave radiation also increased by 6 W m^{-2} due to the rising glacier surface temperature; the net effect is the 14.0 W m^{-2} increase in net longwave radiation. Thus, the driver we emphasize is the increase in incoming longwave radiation, not net longwave radiation — the former being the physically direct and active energy input.

Based on the actual contributions of the three factors, we have reordered the drivers in the abstract and conclusions to: increased incoming longwave radiation, enhanced sensible heat flux, and reduced albedo. All three collectively drove the extreme melt event, with incoming longwave radiation and sensible heat flux serving as direct energy inputs, and reduced albedo acting as a positive feedback that further accelerated the melt.

We have revised the corresponding descriptions in the abstract, the conclusions, and Section 5.3 accordingly, and have also updated Figures 6 and S5.

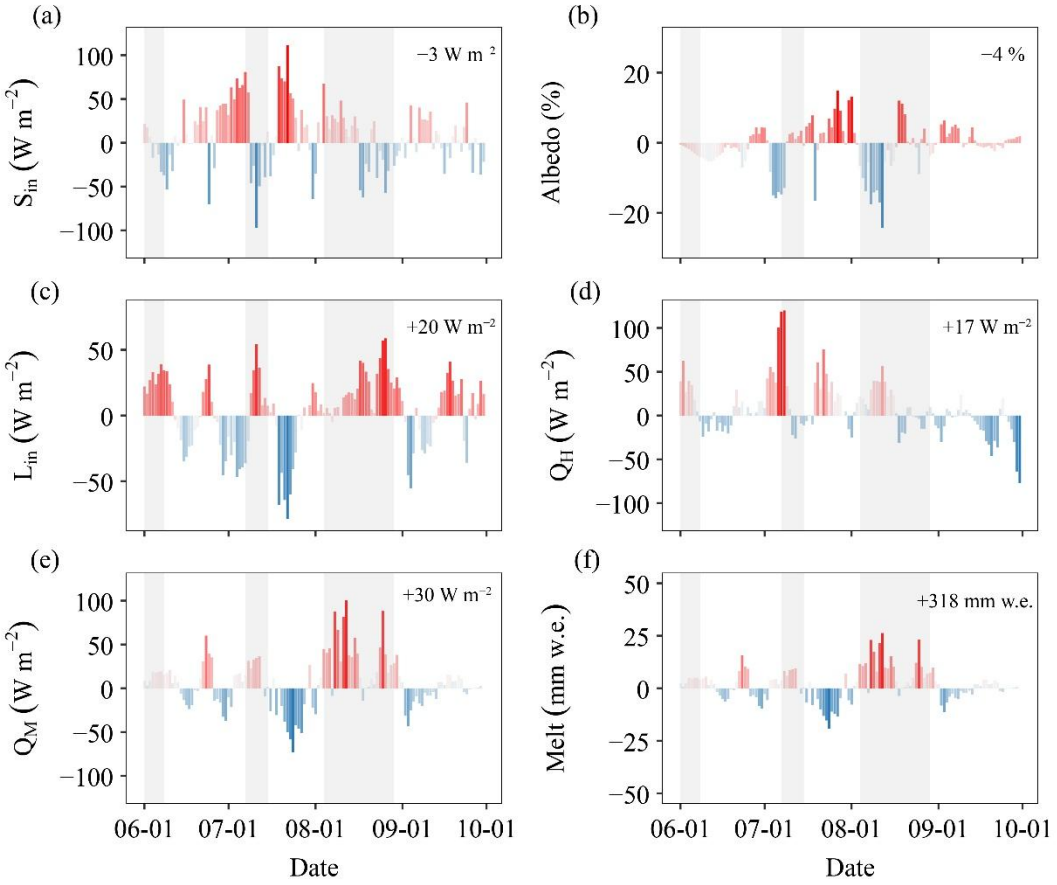


Figure 6. Glacier-wide energy balance anomalies associated with the extreme melt events. Anomalies in (a) incoming shortwave radiation, (b) albedo, (c) incoming longwave radiation, (d) sensible heat flux, (e) melt energy, and (f) melt amount are shown relative to the reference period October 2019–September 2021. Gray shading indicates the 2022 summer heatwave period (June–September).

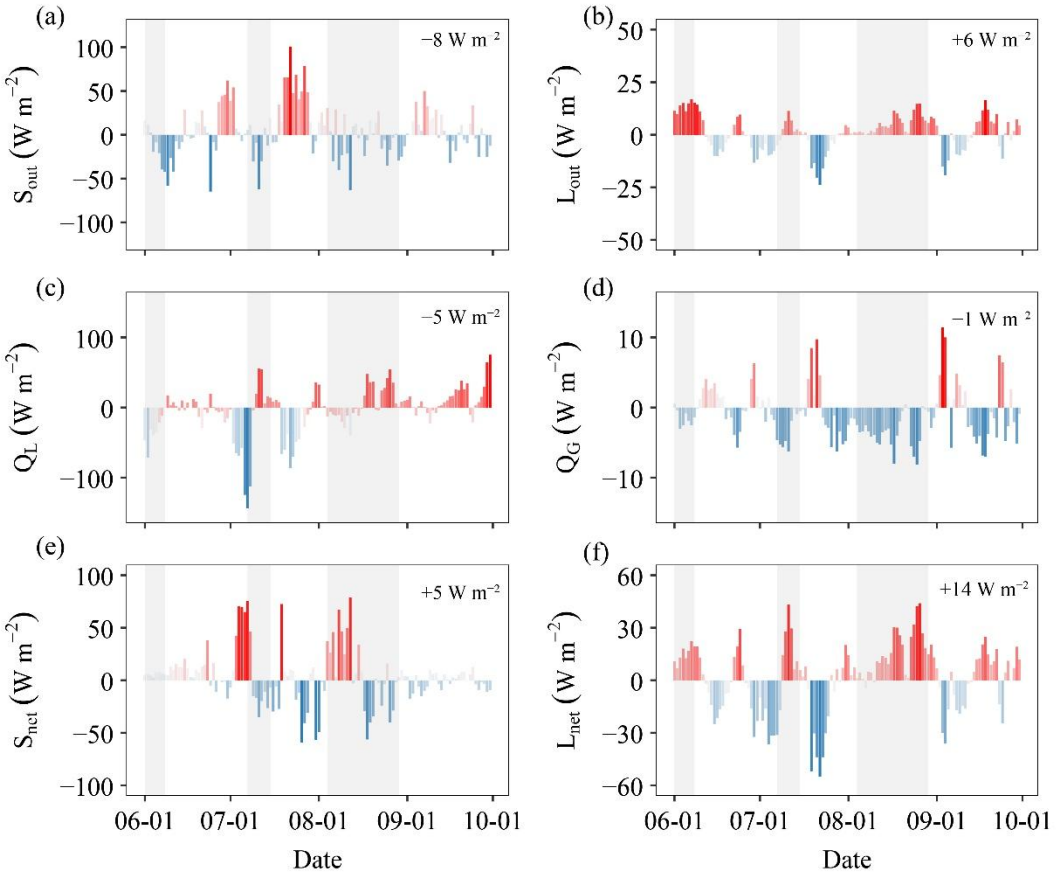


Figure S5. Glacier-wide energy balance anomalies associated with the extreme melt events. Anomalies in (a) outgoing shortwave radiation, (b) outgoing longwave radiation, (c) latent heat flux, (d) snow/ice heat flux, (e) net shortwave radiation, and (f) net longwave radiation are shown relative to the reference period October 2019–September 2021. Gray shading indicates the 2022 summer heatwave period (June–September).

Comment13: Somehow, I cannot reproduce the energy balance numbers. Snet + Lnet + QH + QL + QG = 5.1 + 14.0 + 17.0 - 4.8 - 5.0 = 26.3 W/m2, but the paper reports melt energy increased by 30.7 W/m2.

Response: We thank the reviewer for the careful cross-check. Upon verification, we identified a typo in the anomaly value of QG in the original manuscript. The correct anomaly values for each component are: Snet +5, Lnet +14, QH +17, QL −5, and QG

−1 W m^{-2}, which sum to 30 W m^{-2}. We have corrected the QG value and the corresponding total in the revised manuscript.

Comment14: Link to atmospheric circulation is descriptive, not statistically shown.

• No correlation or regression is shown between the circulation index (or WPSH position) and the actual local melt/albedo/QH anomalies from Section 5.3. The analyses are not statistically connected, why?

• Most importantly, the paper has data for 2 other, non-extreme years but never checks whether the circulation pattern was weaker or different in those years. This comparison seems very doable with what they already have, and would be the clearest way to show the circulation pattern really explains why 2022 was extreme and not just a description of a generally warm TP summer.

Response: We thank the reviewer for raising these two closely related questions. In response to the concerns that "the circulation analysis remains descriptive and lacks statistical validation" and that "no comparison was made with non-extreme years," we have added three lines of supplementary evidence in the revised manuscript, as detailed below.

It should first be noted that the heatwave events identified in this study are concentrated in June–August (the three heatwave windows are 1–8 June, 7–15 July, and 4–29 August). Accordingly, the circulation–heatwave statistical analyses focus on the June–August period, with circulation indices averaged over the same period for interannual correlation analysis.

(1) Spatial characteristics of circulation anomalies

Figure 7a presents the 200 hPa geopotential height and wind anomalies during the 2022 summer heatwave. Relative to the 1992–2021 climatology, an anomalous anticyclone dominated the TP and the regions to its east. The associated subsidence favored atmospheric warming, creating large-scale conditions conducive to the onset,

persistence, and development of the heatwave. Meanwhile, the 12,520 gpm contour of the SAH extended markedly eastward in 2022, indicating a pronounced eastward shift and intensification of the SAH. As one of the most important upper-tropospheric circulation systems over the plateau and its surrounding regions, changes in the SAH's intensity and position can substantially regulate regional vertical motion and thermal structure.

During the same period, an anomalous anticyclone prevailed over Europe, while cyclonic anomalies occurred over the Mongolian Plateau, forming a clear cross-Eurasian circulation pattern (Fig. 7a). Jiang et al. (2024) demonstrated that low soil moisture over the TP can excite an equivalent barotropic anticyclone north of the plateau, which coincides with the subtropical westerly jet waveguide and initiates circumglobal Rossby waves propagating both westward and eastward, ultimately inducing synchronous extreme heatwaves over Europe and East Asia through enhanced downward solar radiation and adiabatic subsidence. Thus, the anomalous anticyclone over the TP in 2022 may not have been merely a local response but rather part of a planetary-scale teleconnection across Eurasia.

(2) Statistical relationship between circulation indices and heatwave intensity

To quantify the effects of these circulation anomalies on the heatwave and extreme melt over the central TP, we analyzed two indices: the Westerly Intensity Index (GTI) and the SAH north–south displacement index (NSI). Following Ding and Wang (2005), we defined the GTI as the standardized anomaly of the 200 hPa geopotential height averaged over 35°–40°N, 60°–70°E, multiplied by –1 so that positive values correspond to enhanced mid-latitude westerlies and enhanced wave-train activity over Eurasia (see also Mölg et al., 2017; Zhu et al., 2024; Fan et al., 2026). Following Wei et al. (2012), NSI is calculated as the difference in mean 200 hPa geopotential height between a northern region (27.5–32.5°N, 50–100°E) and a southern region (22.5–27.5°N, 50–100°E), and then standardized. Positive values indicate a northward displacement of the SAH center and negative values a southward displacement.

Figure 7b shows that GTI was –0.117 in 2022, indicating weakened mid-latitude westerlies. This weakening likely suppressed the southward transport of cold air from higher latitudes and favored the persistence of high-pressure systems. Figure 7c shows that the NSI reached 2.123 in 2022, reflecting a pronounced northward shift of the SAH and enhanced anticyclonic control over the TP. This pronounced northward shift is consistent with the findings of Wang et al. (2024), who demonstrated that an intensified SAH, particularly when coupled with a weakened East Asian jet, significantly increases the frequency of summer high-temperature extremes over the TP. Thus, the anomalous NSI value in 2022 points to a circulation configuration that is statistically conducive to extreme heat. The combined effect of weakened westerlies and an anomalously northward-displaced SAH shaped the upper-level circulation during the 2022 summer heatwave. Through anomalous subsidence and tropospheric warming, this configuration created favorable conditions for the heatwave and the extreme glacier melt.

To quantitatively assess the statistical influence of large-scale circulation on heatwave intensity over the central TP, we calculated Pearson correlation coefficients between summer (June–August) GTI, NSI, and SHI for 1992–2022 (Fig. 8). Based on ERA5 gridded data, GTI was generally negatively correlated with SHI across the central and eastern TP, whereas NSI was generally positively correlated with SHI (Figs. 8a, 8c). These patterns agree with observations at the Tuotuohe meteorological station, indicating that both circulation factors exert significant control on local heatwave intensity. Station observations confirmed these relationships: GTI was significantly negatively correlated with SHI ($r = -0.5$, $p < 0.05$), while NSI was significantly positively correlated with SHI ($r = 0.42$, $p < 0.05$) (Figs. 8b, 8d). In 2022, a negative GTI (–0.117), a strongly positive NSI (2.123), and high SHI values (1.782 for ERA5, 1.684 for Tuotuohe) occurred simultaneously, suggesting a synergistic warming effect of weakened mid-latitude westerlies and a northward-displaced SAH. The consistency between gridded and station data further highlights the significance and statistical robustness of the 2022 circulation anomalies.

(3) Comparison of circulation configurations between 2022 and the non-extreme years of 2020–2021

To assess the uniqueness of this circulation configuration, we compared 2022 with the non-extreme years of 2020 and 2021 using the indices listed in Table 1.

Table 1. June–August SHI and circulation indices for 2020–2022

Year	SHI (ERA5)	SHI(tuotuohe)	GTI	NSI
2020	1.666	-	-1.254	-0.033
2021	1.863	1.288	0.361	0.244
2022	1.782	1.684	-0.117	2.123

Note: Negative GTI indicates weaker westerlies; positive NSI indicates northward displacement of the SAH.

From Table 1, the following observations can be made:

(1) The NSI in 2022 (2.123) is substantially higher than in 2020 (–0.033) and 2021 (0.244), indicating a significant northward shift of the SAH center during the summer of 2022.

(2) The GTI exhibited different states across the three years: –0.117 in 2022 (weakly negative), +0.361 in 2021 (near-climatological), and –1.254 in 2020 (substantially weaker). Despite 2020 having the weakest westerlies among the three years, its NSI was close to climatology (–0.033), lacking the subsidence enhancement from a northward-shifted SAH, and thus its heatwave intensity (SHI = 1.666) was lower than in 2022 (SHI = 1.782). This indicates that the extremity of 2022 cannot be attributed solely to weakened westerlies; rather, it arose from the synergistic combination of weakened westerlies and an anomalously northward-shifted SAH.

(3) The Tuotuohe station SHI in 2022 (1.684) was substantially higher than in 2021 (1.288), while the ERA5 grid data show that 2022 (1.782) was slightly lower than 2021 (1.863). This discrepancy may arise because the ERA5 grid data (0.25°) smooth local topographic effects over complex terrain, whereas the Tuotuohe station, as a point observation, more realistically reflects the response of local thermal conditions to circulation anomalies.

(4) Overall, the circulation configuration in 2022 (weakened westerlies plus an anomalously northward-shifted SAH) was not simultaneously present in 2020 or 2021. The extremity of 2022 was therefore not a result of a generally warm summer, but rather of a specific combination of large-scale circulation anomalies, consistent with the energy flux anomalies documented in Section 5.3.

(4) Coupled feedback between large-scale circulation anomalies and local processes

These large-scale circulation anomalies also influenced the heatwave through land-surface processes. During the summer heatwave, increased cloud cover and enhanced downward longwave radiation promoted near-surface warming (Figs. S8a–c). This warming was accompanied by higher soil temperatures and enhanced evapotranspiration, which reduced soil moisture (Figs. S8e, S8f). However, soil drying may not simply be a passive response to atmospheric forcing; through land–atmosphere interactions, it may in turn modulate the atmospheric circulation. In addition, a drier land surface enhances upward sensible heat flux (Fig. S8d), warming the troposphere and favoring the maintenance of anomalous high-pressure systems (Jiang et al., 2023). This process provides local thermodynamic conditions for the persistence of heatwaves. Therefore, large-scale circulation anomalies may not only directly trigger heatwaves but also prolong and intensify them through a positive feedback involving soil drying, enhanced sensible heating, and high-pressure maintenance (Gui et al., 2024).

An increasing number of studies have shown that large-scale circulation anomalies are important external drivers of extreme glacier mass loss, affecting both surface energy balance and mass balance. Regarding the energy balance, Zhu et al. (2024a) found that clear-sky conditions under anomalous anticyclonic control can enhance incoming shortwave radiation. Simultaneously, higher air temperatures and drier soils can increase sensible heat flux, jointly providing additional energy for glacier melt. In terms of mass balance, warming can shift precipitation from snow to rain, weakening the role of fresh snow in maintaining high glacier albedo. Reduced albedo subsequently increases shortwave radiation absorption and accelerates mass loss (Zhu et al., 2018).

In addition, circulation-induced reductions in moisture transport and precipitation can further limit snow accumulation during the melt season, exacerbating albedo decline and glacier mass loss (Luo et al., 2026). Together, these studies reveal the mechanisms through which large-scale circulation anomalies drive extreme glacier mass loss.

These findings are consistent with our results on the anomalous circulation configuration and the associated extreme melt in 2022, and they support the proposed mechanism whereby weakened mid-latitude westerlies, SAH anomalies, and local energy balance anomalies collectively cause extreme glacier melt. In summary, the extreme glacier ablation during the 2022 summer heatwave was not driven by a single circulation factor. Instead, it resulted from the combined effects of weakened mid-latitude westerlies and the anomalous northward and eastward extension of the SAH. This circulation configuration may have been maintained through planetary-scale teleconnections across Eurasia and further amplified through coupling with soil moisture, sensible heat flux, and radiative processes. These interactions ultimately produced pronounced anomalies in glacier surface energy and mass balance. Our findings advance the understanding of how large-scale circulation affects glacier mass balance over the TP (Yao et al., 2012; Mölg et al., 2014; Zhou et al., 2025; Zhu et al., 2026b) and demonstrate that studies of extreme glacier melt should consider the coordinated effects of tropical and extratropical circulation systems, as well as their coupling with local land-surface processes.

We have rewritten this section and placed it in Section 5.4.

Large-scale circulation anomalies can substantially influence changes in glacier mass balance over the TP and its surrounding regions by modulating regional air temperature and precipitation (Yao et al., 2012; Mölg et al., 2014). The Indian monsoon and the mid-latitude westerlies are the two dominant circulation systems affecting the plateau's climate. Our results indicate that the eastward extension and northward displacement of the SAH, along with weakened mid-latitude westerlies, formed the critical circulation background for the 2022 summer heatwave and the associated

extreme glacier melt event.

Figure 7a presents the 200 hPa geopotential height and wind anomalies during the 2022 summer heatwave. Relative to the 1992–2021 climatology, an anomalous anticyclone dominated the TP and the regions to its east. The associated subsidence favored atmospheric warming, creating large-scale conditions conducive to the onset, persistence, and development of the heatwave. Meanwhile, the 12,520 gpm contour of the SAH extended markedly eastward in 2022, indicating a pronounced eastward shift and intensification of the SAH. As one of the most important upper-tropospheric circulation systems over the plateau and its surrounding regions, changes in the SAH's intensity and position can substantially regulate regional vertical motion and thermal structure.

During the same period, an anomalous anticyclone prevailed over Europe, while cyclonic anomalies occurred over the Mongolian Plateau, forming a clear cross-Eurasian circulation pattern (Fig.7a). Jiang et al. (2024) demonstrated that low soil moisture over the TP can excite an equivalent barotropic anticyclone north of the plateau, which coincides with the subtropical westerly jet waveguide and initiates circumglobal Rossby waves propagating both westward and eastward, ultimately inducing synchronous extreme heatwaves over Europe and East Asia through enhanced downward solar radiation and adiabatic subsidence. Thus, the anomalous anticyclone over the TP in 2022 may not have been merely a local response but rather part of a planetary-scale teleconnection across Eurasia.

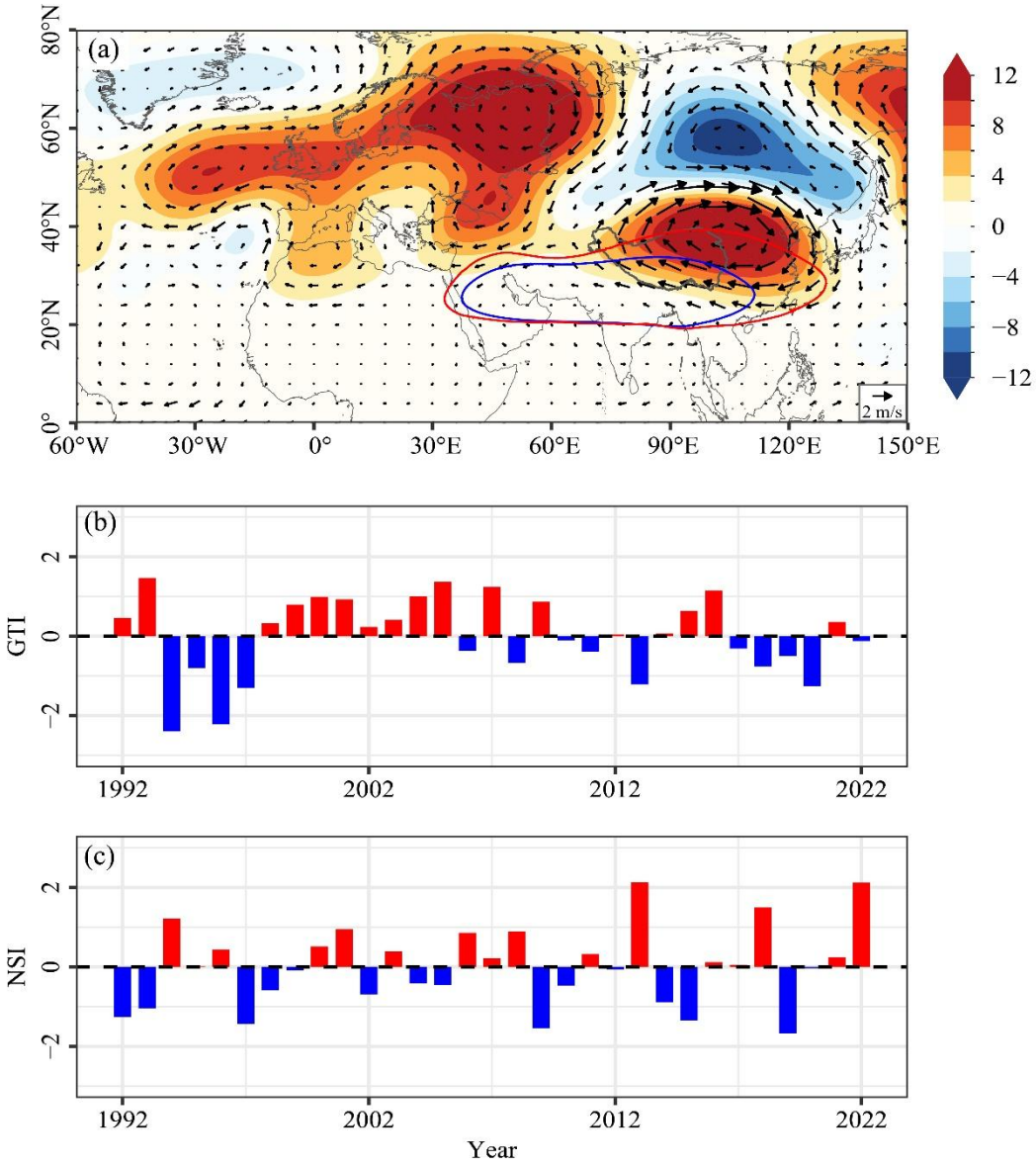


Fig. 7. (a) 200-hPa geopotential height anomalies (shading) and wind anomalies (vectors) during the 2022 summer heatwave, relative to the 1992–2021 climatology; blue and red contours denote the 12,520-gpm isolines for the 1992–2021 climatology and the summer of 2022, respectively, indicating the position and extent of the SAH. (b) Time series of the summer (June–August) GTI from 1992 to 2022; positive values represent enhanced mid-latitude westerly circulation, while negative values represent weakened westerly circulation. (c) Time series of the summer NSI from 1992 to 2022; positive values indicate a northward shift of the SAH, and negative values indicate a southward shift.

To quantify the effects of these circulation anomalies on the heatwave and extreme melt over the central TP, we analyzed the Global Wave Train Index (GTI) and the SAH north–south displacement index (NSI). Following Ding and Wang (2005), we defined the GTI as the standardized anomaly of the 200 hPa geopotential height averaged over 35°–40°N, 60°–70°E. To facilitate interpretation in the context of this study, we multiply this index by –1 (see also Mölg et al., 2017) so that positive values correspond to enhanced mid-latitude westerlies and enhanced wave-train activity over Eurasia. This index has also been applied in previous studies examining the relationship between glacier mass balance and large-scale circulation over the TP and its surrounding regions (Zhu et al., 2024a; Fan et al., 2026). Following Wei et al. (2012), NSI is calculated as the difference in mean 200 hPa geopotential height between a northern region (27.5–32.5°N, 50–100°E) and a southern region (22.5–27.5°N, 50–100°E), and then standardized. Positive values indicate a northward displacement of the SAH center and negative values a southward displacement. Figure 7b shows that GTI was –0.12 in 2022, indicating weakened mid-latitude westerlies. This weakening likely suppressed the southward transport of cold air from higher latitudes and favored the persistence of high-pressure systems. Figure 7c shows that the NSI reached 2.12 in 2022, reflecting a pronounced northward shift of the SAH and enhanced anticyclonic control over the TP. This pronounced northward shift is consistent with the findings of Wang et al. (2024), who demonstrated that an intensified SAH, particularly when coupled with a weakened East Asian jet, significantly increases the frequency of summer high-temperature extremes over the TP. Thus, the anomalous NSI value in 2022 points to a circulation configuration that is statistically conducive to extreme heat. The combined effect of weakened westerlies and an anomalously northward-displaced SAH shaped the upper-level circulation during the 2022 summer heatwave. Through anomalous subsidence and tropospheric warming, this configuration created favorable conditions for the heatwave and the extreme glacier melt.

The statistical relationship between large-scale circulation and heatwave intensity over the central TP was further evaluated through Pearson correlation coefficients between summer (June–August) GTI, NSI, and SHI for 1992–2022 (Fig. 8). Based on

ERA5 gridded data, GTI was generally negatively correlated with S_{HI} across the central and eastern TP, whereas NSI was generally positively correlated with S_{HI} (Figs. 8a, 8c). These patterns agree with observations at the Tuotuohe meteorological station, indicating that both circulation factors exert significant control on local heatwave intensity. Station observations confirmed these relationships: GTI was significantly negatively correlated with SHI (r = –0.5, p < 0.05), while NSI was significantly positively correlated with SHI (r = 0.42, p < 0.05) (Figs. 8b, 8d). In 2022, a negative GTI, a strongly positive NSI, and high S_{HI} values occurred simultaneously, suggesting a synergistic warming effect of weakened mid-latitude westerlies and a northward-displaced SAH. The consistency between gridded and station data further highlights the significance and statistical robustness of the 2022 circulation anomalies.

We further examined the uniqueness of this circulation configuration by comparing 2022 with the non-extreme years of 2020 and 2021 using the indices shown in Figure 7 and Table S5. The NSI in 2022 reached 2.123, far exceeding the values in 2020 (−0.033) and 2021 (0.244), confirming a remarkably northward-displaced SAH during summer 2022. In terms of the GTI, 2022 was negative (−0.117), whereas 2021 showed a positive value (0.361). Notably, 2020 exhibited the most negative GTI (−1.254) among the three years, yet its SHI (1.666) remained lower than that of 2022 (1.782), because its NSI was also negative (−0.033), indicating no northward shift of the SAH. Similarly, although the ERA5-based SHI for 2021 (1.863) slightly exceeded that of 2022 (1.782), the Tuotuohe station SHI for 2021 (1.288) was substantially lower than in 2022 (1.684). More importantly, the NSI in 2021 (0.244), like that in 2020 (−0.033), remained far below the exceptional 2022 value (2.123), indicating that in neither non-extreme year did the SAH exhibit the strong northward displacement observed in 2022. Collectively, these comparisons demonstrate that the extremity of 2022 cannot be attributed to weakened westerlies alone; instead, it arose from the synergistic combination of a negative GTI and a strongly positive NSI (Figure 7c, 7d).

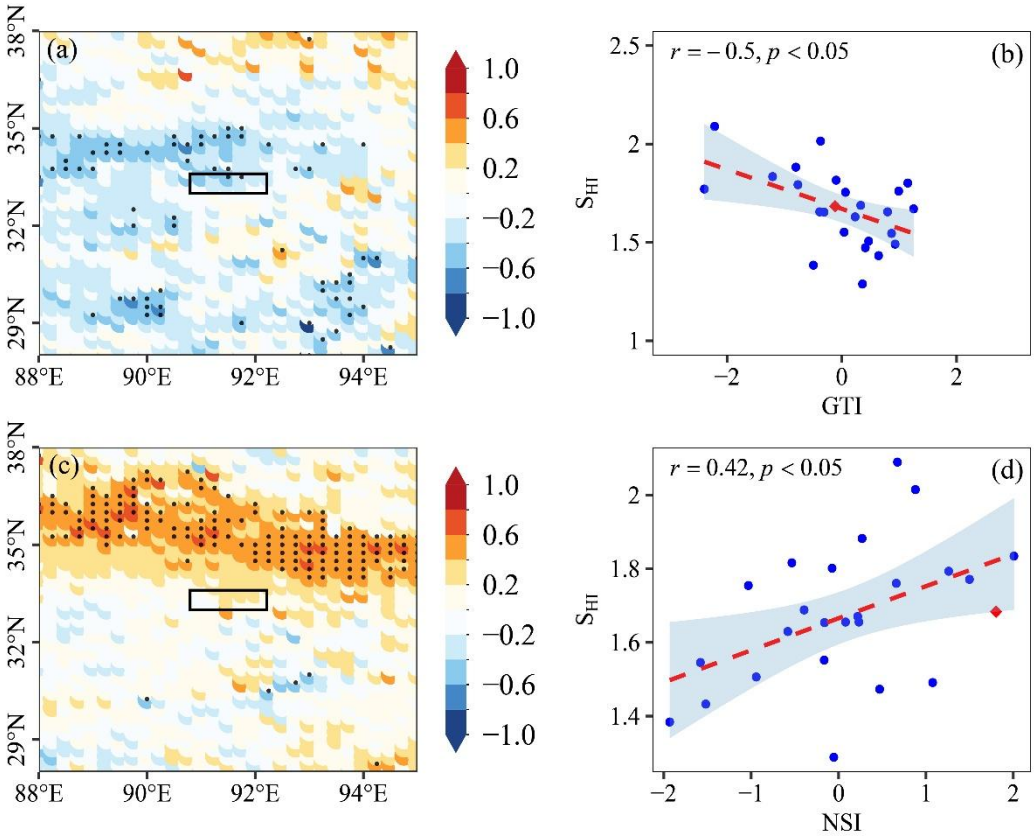


Fig. 8. Correlations between GTI, NSI and SHI during June–August from 1992 to 2022. (a, c) Spatial distribution of correlation coefficients of GTI and NSI with SHI based on ERA5 gridded data; stippling indicates significance at the 95% confidence level ($p < 0.05$). (b, d) Scatter plots and correlation coefficients between GTI/NSI and the SHI calculated from the Tuotuohe meteorological station.

These large-scale circulation anomalies also influenced the heatwave through land-surface processes. During the summer heatwave, increased cloud cover and enhanced downward longwave radiation promoted near-surface warming (Figs. S8a–c). This warming was accompanied by higher soil temperatures and enhanced evapotranspiration, which reduced soil moisture (Figs. S8e, S8f). However, soil drying may not simply be a passive response to atmospheric forcing; through land–atmosphere interactions, it may in turn modulate the atmospheric circulation. In addition, a drier land surface enhances upward sensible heat flux (Fig. S8d), warming the troposphere and favoring the maintenance of anomalous high-pressure systems (Jiang et al., 2023). This process provides local thermodynamic conditions for the persistence of heatwaves. Therefore, large-scale circulation anomalies may not only directly trigger heatwaves

but also prolong and intensify them through a positive feedback involving soil drying, enhanced sensible heating, and high-pressure maintenance (Gui et al., 2024).

An increasing number of studies have shown that large-scale circulation anomalies are important external drivers of extreme glacier mass loss, affecting both surface energy balance and mass balance. Regarding the energy balance, Zhu et al. (2024a) found that clear-sky conditions under anomalous anticyclonic control can enhance incoming shortwave radiation. Simultaneously, higher air temperatures and drier soils can increase sensible heat flux, jointly providing additional energy for glacier melt. In terms of mass balance, warming can shift precipitation from snow to rain, weakening the role of fresh snow in maintaining high glacier albedo. Reduced albedo subsequently increases shortwave radiation absorption and accelerates mass loss (Zhu et al., 2018). In addition, circulation-induced reductions in moisture transport and precipitation can further limit snow accumulation during the melt season, exacerbating albedo decline and glacier mass loss (Luo et al., 2026). Together, these studies reveal the mechanisms through which large-scale circulation anomalies drive extreme glacier mass loss.

These findings are consistent with our results on the anomalous circulation configuration and the associated extreme melt in 2022, and they support the proposed mechanism whereby weakened mid-latitude westerlies, SAH anomalies, and local energy balance anomalies collectively cause extreme glacier melt. In summary, the extreme glacier ablation during the 2022 summer heatwave was not driven by a single circulation factor. Instead, it resulted from the combined effects of weakened mid-latitude westerlies and the anomalous northward and eastward extension of the SAH. This circulation configuration may have been maintained through planetary-scale teleconnections across Eurasia and further amplified through coupling with soil moisture, sensible heat flux, and radiative processes. These interactions ultimately produced pronounced anomalies in glacier surface energy and mass balance. Our findings advance the understanding of how large-scale circulation affects glacier mass balance over the TP (Yao et al., 2012; Mölg et al., 2014; Zhou et al., 2025; Zhu et al., 2026b) and demonstrate that studies of extreme glacier melt should consider the coordinated effects of tropical and extratropical circulation systems, as well as their

coupling with local land-surface processes.

Minor comments

Comment15: The AWS is at 5,700 m, closer to the lower/middle part of the glacier (range 5,400-6,104 m), worth stating clearly that it may not represent the upper part well.

Response: In addition, the AWS was installed at 5,700 m a.s.l., closer to the lower–middle part of the glacier (5,400–6,104 m), and may therefore not fully represent conditions in the upper glacier. We extrapolate point observations to the entire glacier using a temperature lapse rate of 0.6°C per 100 m and a precipitation gradient, with the associated uncertainties quantified through sensitivity analyses (Tables S2–S4). Importantly, because any bias arising from the single-AWS location is systematic across years, it largely cancels out in the interannual comparisons that underpin our identification of the 2021/22 extreme event.

In Section 6.2, which covers the study limitations, we state the uncertainties as follows:

The AWS was deployed at only a single elevation point (5,700 m a.s.l.) on the glacier surface, which is closer to the lower–middle part of the glacier (elevation range 5,400–6,104 m) and may not fully represent conditions in the upper glacier.

Comment16: Point-scale RMSE (288 mm w.e.) is fairly large!

Response: We thank the reviewer for this observation. We fully acknowledge that the point-scale RMSE of 288 mm w.e. is relatively large, and we would like to clarify several points.

First, such a magnitude of point-scale uncertainty is common in distributed glacier mass balance modelling under data-scarce conditions. Point-scale stake measurements represent local information at specific sites, whereas the model outputs are grid-cell

averages at 100 m resolution, and this scale mismatch inevitably introduces differences. In addition, local snow redistribution and micro-topographic features (e.g., undulations, shading) can significantly affect point-scale mass balance, but distributed models operating at 100 m resolution are unable to capture these fine-scale processes fully.

Second, despite the relatively large RMSE at the point scale, the model achieves a correlation coefficient of R = 0.90 (Fig. 2e), indicating that it captures the spatial pattern of mass balance with elevation well. The errors are largely systematic rather than random.

More importantly, our core conclusion—the identification of 2021/22 as an extreme mass loss year—relies on glacier-wide mass balance, not on point-scale values. When aggregated to the glacier scale, random errors cancel out substantially, reducing the RMSE to 101 mm w.e. (Fig. 2g), demonstrating that the model is reliable at the scale relevant to our conclusions.

In Section 6.2, which covers the study limitations, we state the uncertainties as follows:

While the EBFM performs well at the glacier-wide scale, discrepancies are evident at finer scales (point and seasonal), reflecting inherent challenges of distributed glacier modeling under data-scarce conditions. These deviations arise from spatial extrapolation of meteorological variables using simplified lapse rates and gradients, parameterization uncertainty (with albedo and temperature lapse rate being the most sensitive parameters), scale mismatch between point stakes and grid-cell averages, and observational uncertainties in density assumptions and stake height readings.

Comment17: Date ranges for the 3 heatwaves differ slightly across the 3 datasets used (station, ERA5 at station, ERA5 at glacier). A small table showing all 3 ranges and the final overlap would be clearer than relying only on Fig. 3g.

Response: We thank the reviewer for this excellent suggestion. To improve clarity, we have updated Fig. 3g to include the onset and end dates of the three identified heatwave events directly in the figure, allowing readers to see both the overlapping period and

the event timing at a glance. We believe this visual presentation is more effective than a separate table and helps readers quickly grasp the temporal range of each heatwave, while the figure also clearly shows how the three datasets converge on the overlapping periods. We trust this revision adequately addresses the reviewer's concern.